TAMPEREEN TEKNILLINEN YLIOPISTO
TAMPERE UNIVERSITY OF TECHNOLOGY

MIKKO TOIVONEN

LASER BIAS CONTROL FOR A MICRONODE TRANSMITTER

Master of Science thesis

Examiners: Prof. Mikko Valkama and D.Sc (Tech.) Olli-Pekka Lundén
Examiners and topic approved by the
Faculty Council of the Faculty of Computing and Electrical Engineering
on 9th March 2016

ABSTRACT

MIKKO TOIVONEN: Laser Bias Control for a Micronode Transmitter
Tampere University of Technology
Master of Science Thesis, 55 pages
April 2016
Master's Degree Programme in Electrical Engineering
Major: Wireless Communications
Examiners: Professor Mikko Valkama and D.Sc. (Tech.) Olli-Pekka Lundén

Keywords: Radio Frequency over Glass, RF detector, optics, bias

Radio frequency over glass (RFoG) is a fiber-to-the-home (FTTH) network. An RFoG network is essentially a hybrid fiber coaxial (HFC) network, whose coaxial portion has been replaced with a passive point-to-multipoint optical network. Thus, the fiber is brought all the way to subscriber homes. Downstream and upstream transmissions share the same optical fiber, which is enabled by wavelength division multiplexing. The downstream and upstream signals are transmitted using semiconductor lasers with wavelengths of 1550 nm, and 1310 or 1610 nm, respectively.

A radio frequency over glass optical networking unit (R-ONU), also called the micronode, is located at customer premises. A micronode is basically an optical-to-electrical converter: its receiver converts optical downstream signals into electrical and its transmitter electrical upstream signals into optical. The downstream signals are continuous, whereas the upstream signals coming in from the home cable modem operate in burst mode. When an upstream signal is not present in the coaxial input, the bias current of the transmitting laser is turned off. The upstream transmitter turns on when an upstream signal coming from the cable modem is detected. On turn-on, the bias current of the laser is switched on and the upstream RF signal is fed to the laser. This will lead to amplitude modulated (AM) optical signal, where the carrier is the optical power of the laser and the modulating signal the upstream RF signal.

The objective of this thesis was to design a concept that enables the burst mode operation of an RFoG micronode upstream transmitter. Different components and electrical architectures were evaluated and compared in order to achieve a design that met the laser turn-on/turn-of requirements of Society of Cable Telecommunications Engineers (SCTE) Radio Frequency over Glass Specification. The specification states that a micronode upstream laser must exhibit turn-on and turn-off times of 1.3 us and 1.6 us, respectively. In addition, the specification sets ranges for input RF powers for which the laser must turn on and off.

The proposed concept was proven to be suitable for an RFoG micronode. The design achieved turn-on and turn-off times of 700 ns and 600 ns, respectively. It is also shown that by utilizing a hysteresis circuit in a voltage comparator, the range of input powers for laser turn-on and turn-off can be adjusted to meet the specification.

Teleste Corporation, for whom this thesis was written, offers a great portfolio in HFC network optical node products. The proposed concept can be used to modify these products in order to achieve a device that could be utilized in an RFoG network.

TIIVISTELMÄ

MIKKO TOIVONEN: Mikrosolmulaitteen laserin biasohjaus
Tampereen teknillinen yliopisto
Diplomityö, 55 sivua
Huhtikuu 2016
Sähkötekniikan diplomi-insinöörin tutkinto-ohjelma
Pääaine: Wireless Communications
Tarkastajat: Professori Mikko Valkama, TkT Olli-Pekka Lundén

Avainsanat: Radio Frequency over Glass, RF detektori, optiikka, biasointi

Radio Frequency over Glass (RFoG) on tietoverkko, jossa valokuitu tuodaan tilaajalle saakka. RFoG-verkko on kuin hybridi-kuitu-koaksiaali-verkko (HFC, hybrid fiber coaxial), jonka koaksiaalinen osuus on korvattu passiivisella optisella verkolla. Meno- ja paluusuunnan lähetykset jakavat saman optisen kuidun hyödyntäen aallonpituusjakoista multipleksointia. Signaalit lähetetään käyttämällä puolijohdelasereita, joiden aallonpituudet menosuunnalle on 1550 nm ja paluusuunnalle joko 1310 tai 1610 nm.

RFoG-verkkoyksikkö (R-ONU, RFoG Networking Unit), jota kutsutaan nimellä mikrosolmulaite, on sijoitettu asiakkaan tiloihin. Mikrosolmulaite on sähköoptinen muunnin: sen vastaanotin muuntaa menosuunnan optisen signaalin sähköiseksi ja sen lähetin paluusuunnan sähköisen signaalin optiseksi. Menosuunnan signaalit ovat jatkuvia, kun taas asiakkaan tiloissa olevan kaapelimodeemin lähettämät paluusuunnan signaalit ovat purskeita. Mikrosolmulaitteen lähettimen laserin biasvirta on katkaistu, kun laitteen koaksiaalisessa sisääntulossa ei ole paluusunnan signaalia. Lähetin kytkeytyy päälle, kun kaapelimodeemilta saapuva paluusuunnan signaali havaitaan. Tällöin laserin biasvirta kytketään päälle ja paluusuunnan RF-signaali ohjataan laserille. Tämä johtaa amplitudimoduloituun (AM) signaaliin, jossa kantoaaltona toimii laserin lähettämä optinen teho ja moduloivana signaalina paluusunnan RF-signaali.

Tämän diplomityön tarkoituksena oli suunnitella konsepti, joka mahdollistaisi RFoG mikrosolmulaitteen paluusuunnan lähettimen toiminnan, kun sisääntuleva signaali on pursketyyppinen. Eri komponentteja ja elektronisia kytkentöjä vertailtiin, jotta aikaansaataisiin laite, joka täyttäisi laserin syttymiseen ja sammumiseen liittyvät vaatimukset. Nämä vaatimukset ovat esitetty Society of Cable Telecommunications Engineers (SCTE) RFoG Spesifikaatiossa. Spesifikaatio määrittelee, että laserin tulee syttyä 1,3 µs:ssa ja sammua 1,6 µs:ssa. Lisäksi spesifikaatio määrittelee sisäänmenotehon alueet, joilla laserin tulee syttyä ja sammua.

Suunniteltu konsepti osoitettiin soveliaaksi RFoG-mikrosolmulaitteeseen. Suunniteltu laite saavutti 700 ns:n syttymis- ja 600 ns:n sammumisajan. Lisäksi osoitettiin, että käyttämällä hystereesipiiriä jännitevertailijassa, laserin syttymiseen ja sammumiseen johtavat sisäänmenotehon alueet saadaan säädettyä siten, että ne täyttävät spesifikaation vaatimukset.

Teleste Oy, jolle tämä diplomityö kirjoitettiin, tarjoaa laajan portfolion verkon optisia solmulaitteita. Tässä työssä esitettyä konseptia voidaan hyväksikäyttää modifioimalla näitä tuotteita siten, että niitä voitaisiin käyttää RFoG-verkossa.

PREFACE

This thesis was written for Teleste corporation. I would like to express my gratitude to Toni Rumpunen for providing me a subject, supervising my work and giving me the opportunity to work in his R&D team.

I wish to thank D.Sc (tech) Olli-Pekka Lundén for his guidance on the scientific writing process. Olli-Pekka's contribution and attention to detail gave me the means to do my best. I feel privileged to have had Olli-Pekka as my teacher, examiner and supervisor. I also wish to thank Professor Mikko Valkama for providing valuable comments and examining this thesis.

To my dear family. Thank you for all the support during my studies and the writing process of this thesis.

Finally, I would like to thank B.Sc. Katariina Tuohimäki for her support.

Rauma, 10.3.2016

Mikko Toivonen

CONTENTS

LIST OF FIGURES

LIST OF SYMBOLS AND ABBREVIATIONS

AC	alternating current
ADC	analog to digital converter
AM	amplitude modulation
CAPEX	capital expenditure
CATV	common antenna television
CMOS	complementary metal oxide semiconductor
CMTS	cable modem termination system
CW	continous wave
dB	decibel
dBmV	a unit of power expressed in dBmV, referenced to 1 mV across 75 ohms
dBuV	a unit of power expressed in dBuV, referenced to 1 µV across 75 ohms
DC	direct current
DFB	distributed feedback
DOCSIS	data over cable service interface specification
DS	downstream
EMC	electromagnetic compatibility
EMI	electromagnetic interference
EPON	ethernet passive optical network
FDD	frequency division duplexing
FET	field effect transistor
FTTx	fiber-to-the-X (eg. home)
GPON	gigabit-capable passive optical networks
HFC	hybrid fiber coaxial
IC	integrated circuit
ITU	International telecommunications union
LASER	light amplification by stimulated emission of radiation
LED	light emitting diode
ODN	optical distribution network
OFDM	orthogonal frequency-division multiplexing
OMI	optical modulation index
PA	power amplifier
QAM	quadrature amplitude modulation
RF	radio frequency
RFoG	radio frequency over glass
RMS	root-mean-square
R-ONU	RFoG optical network unit
RX	receiver
SCTE	Society of cable telecommunications engineers
SNR	signal-to-noise-ratio
TDM	time division multiplexing
TEC	thermoelectric cooler
TX	transmitter
WDM	wavelength division multiplexing
US	upstream

A	closed-loop gain of a negative feedback circuit
A_{ideal}	ideal closed-loop gain of a negative feedback circuit
a	open-loop gain of an operational amplifier or a control circuit
c	speed of light
d	core diameter of an optical fiber
f	frequency
G	closed-loop gain of an operational amplifier circuit
G_{ideal}	closed-loop gain of an ideal operational amplifier circuit
h	Planck's constant
i_n	input current of the inverting input of an operational amplifier
i_p	input current of the non-inverting input of an operational amplifier
n	optical index of a medium
P_{avg}	average optical power of a semiconductor laser under modulation
P_{max}	maximum instantaneous optical power of a semiconductor laser under modulation
P_{min}	minimum instantaneous optical power of a semiconductor laser under modulation
r_d	differential input impedance of an operational amplifier
r_o	output resistance of an operational amplifier
v_d	differential input voltage of an operational amplifier or a comparator
v_n	inverting input or input voltage of an operational amplifier or a comparator
v_p	non-inverting input or input voltage of an operational amplifier or a comparator
β	feedback factor of a control circuit or an operational amplifier
θ_i	angle of incident of a light beam
θ_{rf}	angle of refraction of a light beam
θ_{rl}	angle of reflection of a light beam

1. INTRODUCTION

Cable operators have been utilizing bidirectional hybrid fiber coaxial (HFC) networks for providing internet access, cable telephony, and video services for their customers since the early 1990s. An HFC network utilizes an optical fiber to transport signals between the headend and an optical node [1]. The optical node converts the optical signal to electrical (or electrical to optical in the upstream direction) and feeds it to a coaxial network. A single node can serve multiple coaxial networks. A coaxial network is used to transport the electrical signal between the optical node and the customers using 75 Ω coaxial cables and taps. The use of a coaxial network calls for line extender amplifiers between the optical node and the customer, due to the losses present in the coaxial cables and taps.

Currently, cable operators are pushing the fiber-to-coaxial point of transition closer to the customer premises. This is often called a deep-fiber network. As the optical portion of an HFC network is expanded, the cost of the network is decreased and the reliability is increased due to lower number of active devices in the network [2]. In addition, pushing the optical node closer to the customers leads to more subscribers served per fiber. Thus, the bandwidth per customer is increased.

A potential architecture for pushing the fiber-to-coaxial point of transition closer to the customer is a radio frequency over glass (RFoG) network. An RFoG network allows the fiber to be brought all the way to the customer. An RFoG network is completely compatible with existing headend and customer premises equipment. However, rather than utilizing an optical node, which can serve up to 2000 homes through a coaxial network, an RFoG network utilizes a micronode serving only 1 home (or a few homes in an apartment building). The coaxial cable is only used for in-house wiring. [3]

The technology used for transmitting downstream signals (from headend to customer) is identical in HFC and RFoG networks. However, the situation differs in the upstream (from customer to headend) direction. RFoG uses time division multiplexing (TDM) in the upstream direction, which allows multiple signals to be terminated at a single upstream receiver. This leads to a significant reduction in the number of upstream receivers at the service providers headend.

The nodes used in traditional HFC networks are not designed to utilize TDM. Their transmitting lasers are always on, regardless whether an upstream signal is present. This is not the case with RFoG micronodes. The transmitting laser of a micronode is on only if upstream signal is present. Therefore, the operation of an RFoG micronode relies on

its ability to sense an upstream signal in its coaxial input: the micronode must be able to turn on and off the transmitting laser in the presence or absence of upstream signal [4]. This will serve as motivation for this thesis.

The aim of this thesis is to develop and build a laser control circuit that could be utilized in Teleste corporations future RFoG micronode product. The developed device must be able to turn on and turn off the optical carrier power of the transmitting semiconductor laser in the presence and absence of input RF signal. The scope of this thesis is limited to the on/off switching of the transmitting lasers carrier power. However, the modulation of the laser is addressed by discussion in Chapter 3 in order to give the reader a wider understanding on the technology in question.

According to the SCTE RFoG specification, the realized device must be able to exhibit fast response times. The optical output power of the laser must reach 90 % in 1.3 µs from the application of input RF signal. When the input RF signal is removed from the device input, the optical power must fall to 10% in 1.6 µs.

The process of developing the control circuit consisted of design, comparison of applicable components, and verification measurements. The thesis is organized as follows. The next chapter presents background on hybrid fiber coaxial and radio frequency over glass networks. Chapter 3 discusses background theory on the applied electric and optical components. The design is discussed in Chapter 4. Measurement results are presented in Chapter 5. Chapter 6 gives a brief summary on conclusions and future work.

2. HYBRID FIBER COAXIAL AND RADIO FREQUENCY OVER GLASS NETWORKS

This chapter will present a brief introduction on hybrid fiber coaxial (HFC) and radio frequency over glass (RFoG) networks. In addition, the RFoG optical networking unit (R-ONU) is discussed. In the industry, the R-ONU is usually referred as micronode, which is also the term used in this thesis. This chapter also explains why cable operators would want to deploy an RFoG network instead of an HFC network.

2.1 Hybrid fiber coaxial network

A CATV (common antenna television, community antenna television) network was not intended to be a multipurpose communications mechanism. It only provided one-way analog video transmission through a tree-and-branch coaxial network. The original purpose of these systems was to deliver broadcast signals in areas where sufficient antenna reception was not guaranteed [5, p.5]. The signals were transported from the service providers headend to multiple customers using coaxial cables, RF power amplifiers, power splitters, and directional couplers. Several amplifiers had to be cascaded to overcome the losses present in coaxial cables and passive components. The signal attenuation in a coaxial cable can be in the order of 50 dB / km [6, p.20]. This suggests that an RF amplifier with a gain of 25 dB is required after every 500 meters. Cascading multiple amplifiers result in a degradation of signal quality due to added noise and distortion. The third order distortions increase approximately 6 dB, and the carrier-to-noise ratio decrease 3 dB, when the amount of amplifiers in cascade is doubled [5, p.6]. In addition, cascading multiple amplifiers introduces a reliability hazard: a malfunction in just one amplifier can result in loss of signal for several customers.

Nowadays, the modern hybrid fiber coaxial (HFC) networks enable two-way data transmission. An HFC network is composed of an optical and a coaxial portion and is used to carry broadband content such as video, data, and voice between the headend and the customer. The use of fiber technology has led to a reduced number of cascaded amplifiers due to the low loss nature of optical data transmission in a fiber. This has led to a better signal quality and greater bandwidth [5, p.18]. A typical HFC network is presented in Figure 2.1.

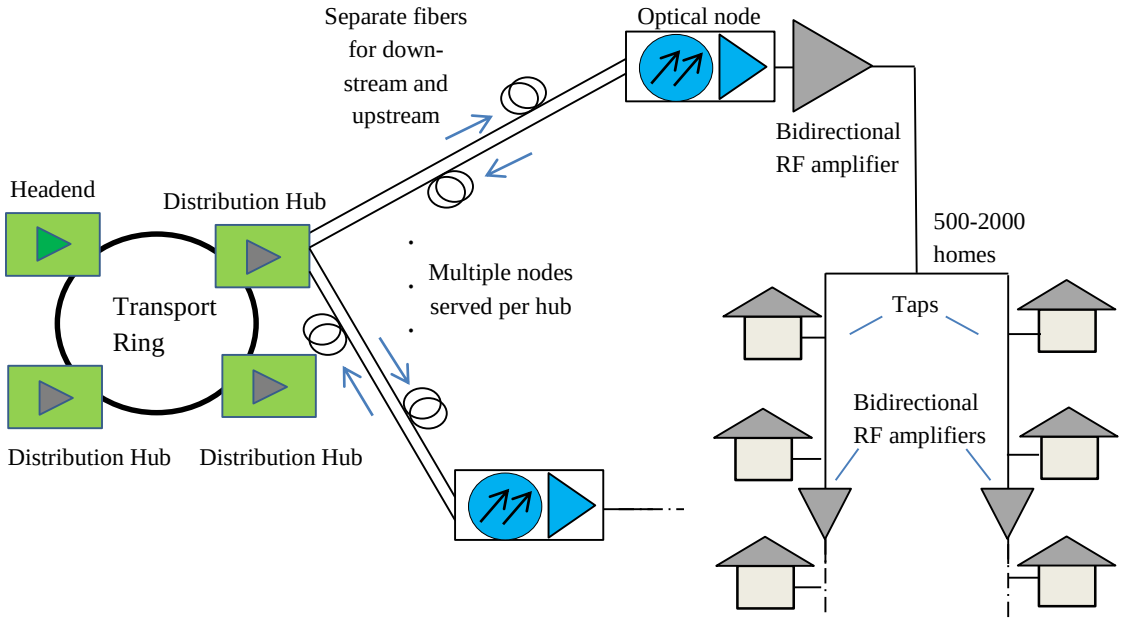

Figure 2.1. *Typical HFC network.*

Considering first the downstream direction, the headend combines data and video signals from satellite transponders, terrestrial broadcast, and video servers using subcarrier multiplexing [6, p.12]. After the multiplexing, the broadband RF signal (for example from 54 MHz to 1002 MHz) is used to modulate the intensity of a semiconductor laser. The headend feeds the optical signal to multiple distribution hubs using a fiber trunkline. The data is then sent from a distribution hub to an optical node through an optical fiber. The optical portion of the HFC network is used to transmit the signals for the long distances, which is 15 - 20 km on average (but can be as high as 40 km) in Europe [7]. The fiber is terminated at the optical node, which converts the optical signal back to electrical RF signal using a photodiode receiver. The electrical signal is then amplified and distributed to the coaxial cable network. The optical node usually contains more than one RF ports. Thus, it can feed multiple coaxial networks. [6, p.14]

Now that the signal is travelling in a coaxial cable, it can be delivered to subscriber homes using taps. A tap is essentially a combination of directional couplers and power splitters [6, pp.15-16]. Line extender amplifiers are inserted in the coaxial network in order to amplify the signal for subscribers located further away from the optical node. Several line extender amplifiers can be cascaded, but with the cost of signal degradation due to increased noise and distortion. In Europe, a maximum of 4-5 amplifiers are typically connected in cascade [7].

The cable section of an HFC network is fully bidirectional. Upstream signals will travel back from the subscriber premises to the optical node using the same coaxial cables, taps, and amplifiers as downstream signals. This is achieved with frequency division duplexing (FDD). Frequency division duplexing is enabled with the use of diplexers in

the bidirectional amplifiers. Figure 2.2 presents a block diagram of a typical HFC network RF amplifier.

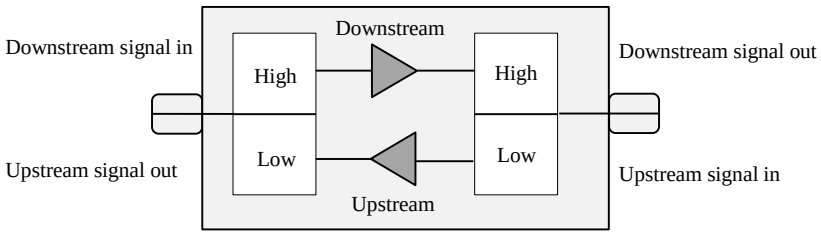

Figure 2.2. *An HFC line amplifier.*

The bidirectional amplifier is equipped with diplexers at both its ports. The diplexers are used to guide the downstream and upstream signals to the correct amplifiers circuits. The "High" side of the diplexer allows signals in downstream band to pass it, whereas the "Low" side of the diplexer allows only signals in the upstream band to pass [6, p.11]. If the downstream and upstream signals were transmitted using same frequencies, separate cables would be needed. With the use of frequency division duplexing, network costs are reduced, because only one cable is needed.

For the new DOCSIS 3.1 (Data Over Cable Service Interface Specification), upstream and downstream frequency bands are 5 – 42 MHz and 54 – 1002 MHz, respectively. However, they are extendable. The upstream frequency band can be extended to upper limits of 65, 85, or 204 MHz. The downstream frequency band can be extended to upper limits of 1218 and 1794 MHz (or even higher in the future). When the upper limit of the upstream is extended, the lower limit of downstream band must be raised to either 108 MHz or 258 MHz, to ensure that the two bands do not overlap [8]. The different configurations are presented in Table 2.1.

Table 2.1. *DOCSIS 3.1 upstream and downstream band configurations.*

Band	**Lower edge**	**Upper edge**	**Optional lower edge**	**Optional upper edge**
Upstream	5 MHz	42 MHz	NA	65, 85, or 204 MHz
Downstream	54 MHz	1002 MHz	108 or 258 MHz	1218 or 1794 MHz

Once the upstream electrical signal encounters the optical node, it is used to modulate a semiconductor laser and the data is transmitted to the headend optically. However, in most cases, the upstream optical signal will not share the same fiber with the downstream signal. [3; 6, p.17]

2.2 Radio frequency over glass network

The trend of evolvement in HFC networks is to push the fiber-to-coaxial point of transition closer to the customer. Radio frequency over glass (RFoG) is a new technology that enables a novel approach to implement a fiber-to-the-home (FTTH) network architecture. In addition, RFoG preserves the traditional HFC equipment in the headend and customer premises, such as the CMTS (cable modem termination system), QAM set-top boxes and DOCSIS cable modems. Instead of the optical nodes utilized in HFC, RFoG uses micronodes that are located in subscriber homes.

Figure 2.3 shows the reference architecture for an RFoG system.

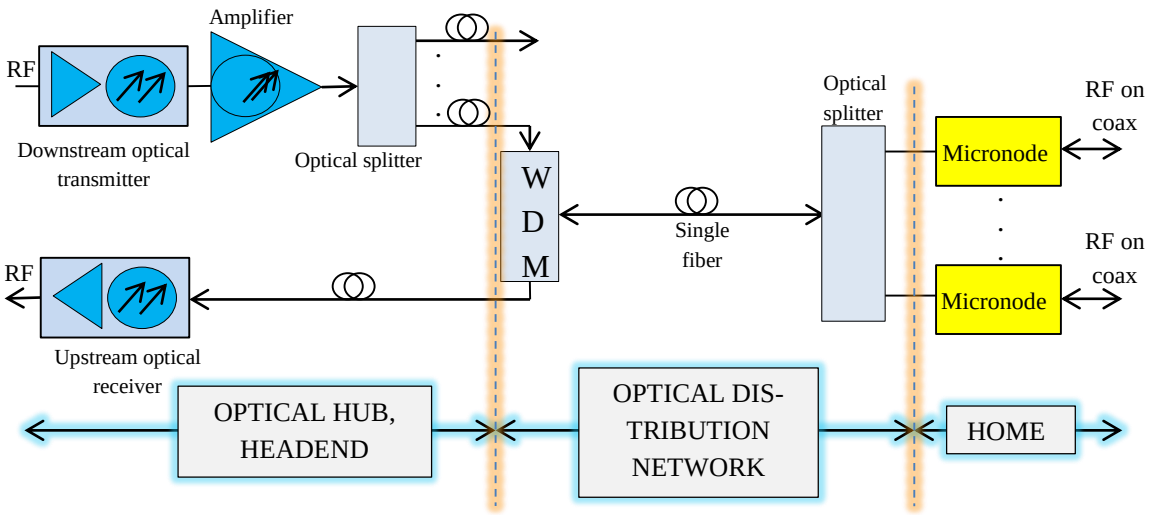

Figure 2.3. *RFoG network. Adopted from [4].*

Located at the headend, the optical hub consists of a downstream optical transmitter, downstream optical amplifier and splitter, and an upstream optical receiver. Downstream operates on a wavelength of 1550 nm, whereas upstream uses either 1310 or 1610 nm. 1310 nm upstream wavelength enables more cost effective solutions due to the wide availability of active and passive components, whereas 1610 nm permits the coexistence of either IEEE 802.ah (EPON) or ITU G.984 (GPON) system, thus being more future-proof [9]. Isolation and multiplexing between the transmitter and receiver of the optical hub is achieved with the wavelength division multiplexer (WDM), which facilitates the interface between the optical hub and the optical distribution network (ODN). Other than the usage of WDM, which allows the downstream and upstream signals travel along the same fiber, the downstream architecture is basically the same as in a HFC network. At the end of the ODN, the signal is split into micronodes using an optical splitter. The micronodes are located either at home (FTTH, fiber-to-the-home), or at a building (FTTB, fiber-to-the-building).

The transmission technology in RFoG differs from HFC in the upstream direction. In RFoG, all micronodes connected to a single optical splitter (maximum split of 1:128) are terminated with a single optical receiver (whereas in HFC every optical node has its dedicated receiver in central station site). This is achieved with time division multiplexing (TDM) of upstream signals and it significantly reduces the amount of upstream receivers in the headend [3].

2.2.1 RFoG micronode

The optical distribution network is terminated at the micronode, which converts the signal from optical to electrical (electrical to optical) in the downstream (upstream) direction. An example of a micronode architecture is presented in Figure 2.4.

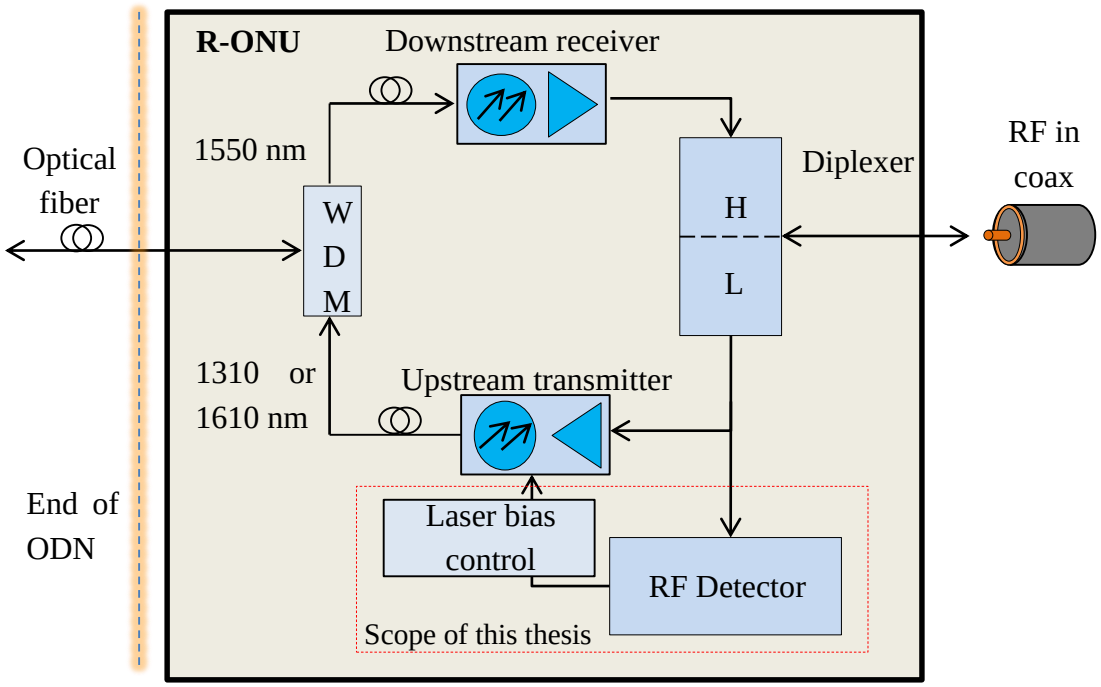

Figure 2.4. *Block diagram of a micronode. Adopted from [4].*

The micronode receives downstream optical signal from the network and couples it to the downstream receiver through the wavelength division multiplexer (WDM). The receiver converts the optical signal into RF using a photodiode. The RF signal is then fed to the coaxial cable through the diplexer. Finally, a cable modem, QAM set-top-box, or a QAM tuner terminates the coaxial cable.

The micronode upstream transmitter operates in burst mode. The transmitter is switched on only when RF power in the upstream band is detected. The TDM-scheme allows signals from multiple upstream transmitters to travel through a single fiber to a single upstream receiver. Without TDM, upstream signals sent from different micronodes to a single receiver would block each other.

2.2.2 Benefits of an RFoG network

An RFoG network benefits from the fact that the fiber is brought all the way to the customer, thus lacking the need of amplifiers and active elements in the field. This leads to CAPEX (capital expenditure) savings, especially in rural areas [9]. The passive optical network that is used to replace the coaxial portion of an HFC network can be constructed using low cost passive components. This leads to more reliable solution and requires less maintenance. For example, a local power outage will not affect the passive optical network. Furthermore, the optical fiber is immune to RF interference, because it is built from non-conducting materials.

A cable operator can also choose an RFoG network over a HFC network, because it is more future proof. RFoG can share the same infrastructure with baseband modulated GPON and EPON internet protocol solutions. They can share the same passive optical network, because their lasers utilize different wavelengths. The wavelengths for the downstream and upstream directions of GPON and EPON are 1490 nm and 1310 nm, respectively. As mentioned earlier, RFoG utilizes a downstream wavelength of 1550 nm. The upstream wavelength can be chosen to be 1610 nm, and thus allowing a GPON/EPON overlay.

3. BACKGROUND THEORY

This chapter will present background theory on the optics, electronic components, and different techniques that dictate the behavior of an RFoG micronode. The discussed background theory will be applied in the proposed design presented in Chapter 4. Some topics that are not included in the scope of this thesis (such as the laser diode modulation) are also discussed. This offers the reader a wider perspective on the technology in hand.

3.1 Reflection and refraction of light

Figure 3.1 presents a situation, where an incident beam of light encounters an interface between two media. A part of the incident beam is reflected and a part is refracted.

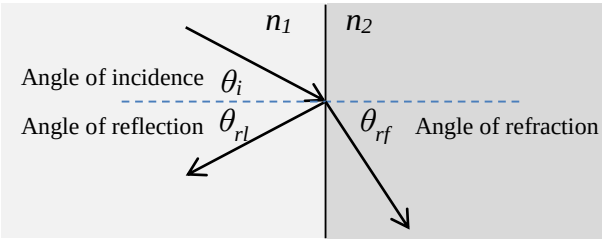

Figure 3.1. *Reflection and refraction of light.*

Laws of reflection and refraction can be expressed in three sentences (assuming monochromatic light):

1. The incident, reflected, and refracted beams of light and the normal of the interface between the two media all lie on the same plane.
2. The angle of reflection θ_{rl} equals the angle of incidence θ_i, that is
$$\theta_{rl} = \theta_i \tag{3.1}$$
3. The relation between the angles of incident θ_i and refraction θ_{rf} is expressed by Snell's law
$$n_1 \sin\theta_i = n_2 \sin\theta_{rf}, \tag{3.2}$$
where n_1 and n_2 are the optical indexes of the different materials in the interface.

As the angle of incidence θ_i increases, the angle of refraction θ_{rf} increases. With a certain incident angle, called the critical angle of incidence, θ_c, the angle of refraction will reach $\theta_{rf} = 90°$. The critical angle can be found with

$$\sin\theta_c = \frac{n_2}{n_1} \tag{3.3}$$

At incident angles equal or greater than θ_c all light will reflect and non is refracted. This is called total internal reflection.[10, p.1252]

3.2 Optical fiber

As presented earlier, the angles of reflection and refraction of light depends on the optical indexes of the respective media as well as the incident angle. An optical fiber utilizes total internal reflection in order to operate as a low loss signal transmission medium. In communications, optical fibers are used to convey a modulated beam of light. An optical fiber does not conduct electricity. Thus, it is immune to electromagnetic interference (EMI): unwanted signals are not able to couple to the system along the optical fiber. Moreover, the losses in an optical fiber are significantly lower than those in coaxial cables. For these reasons, the optical fiber is used increasingly in long distance telephone, television and internet communication.

The optical fiber has three layers called the core, cladding, and coating, as presented in Figure 3.2a.

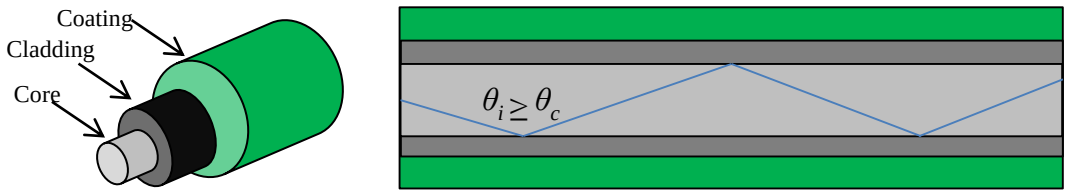

Figure 3.2. *Three layers of the optical fiber. Adopted from [11, p.48].*

The light propagates in the core, while cladding provides the different optical index to achieve total internal reflection. The index of the cladding is only less than 1% lower than the index of the core - for example, typical values for the optical indexes of the core and cladding are 1.47 and 1.46, respectively. While the core and cladding are used to control the propagation of light inside the fiber, the coating is only used to protect the structure from shocks and other mechanical issues that can affect the optical properties of the fiber. [11, pp. 47-48]

Figure 3.2b depicts how light travels inside a multimode optical fiber. Total internal reflection will occur, when the light hits the core-cladding-interface in an angle greater than the critical angle. Because the angles of incident and reflection equal, the next reflection after the previous one will always be a total internal reflection (assuming a slightly or non-bent fiber). However, if the light enters the fiber in a way that the incident angle in the core-cladding-interface is smaller than the critical angle, total internal

reflection will not occur. Now, some of the light passes through the core-cladding-interface, and is refracted. The cladding is usually made from a material with a shallow penetration depth, and therefore, the light attenuates rapidly.

If the light beams are imperfectly collimated (they are not accurately parallel), they can enter a multimode optical fiber in multiple angles. This is depicted in Figure 3.3.

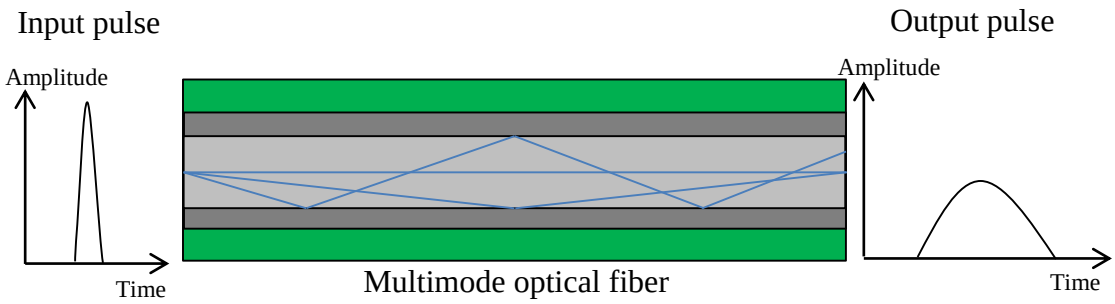

Figure 3.3. *Propagation of light in a multimode optical fiber.*

Light propagating straight along the fiber will travel a smaller distance than light entering in an angle. Thus, the light beam travelling straight along the fiber will reach the other end faster than a light beam which is constantly reflecting along the fiber. Different paths, known as modes, will result to different transmit times. As presented in Figure 3.3, for a pulse input signal, a spread output signal is observed. This mode dependent propagation velocity is called modal dispersion. [5, pp.474-475]

The optical links in an RFoG network can be in the order of several tens of kilometers. The utilization of multimode fibers would lead to severe modal dispersion. Therefore, multimode fibers are omitted and singlemode fibers are used instead. By using a very small core diameter and a very small difference in the refraction indexes of the core and cladding, the modal dispersion is reduced to a point, where the fiber supports only one mode. Only one mode is supported, when

$$V = \frac{2\pi d\sqrt{n_1^2 - n_2^2}}{\lambda} < 2.405\,, \tag{3.4}$$

where V is the normalized frequency, d is the core diameter, n_1 the refractive index of the core, n_2 the refractive index of the cladding, and λ the free-space wavelength of the applied light. [12, p.509]

A single mode fiber allows light to travel only collinearly with its axis. This is known as the LP_{01} mode. Now that the light can only propagate in one mode, modal dispersion is eliminated and the transmitted signal is not distorted, as presented in Figure 3.4 [5, pp.477-478].

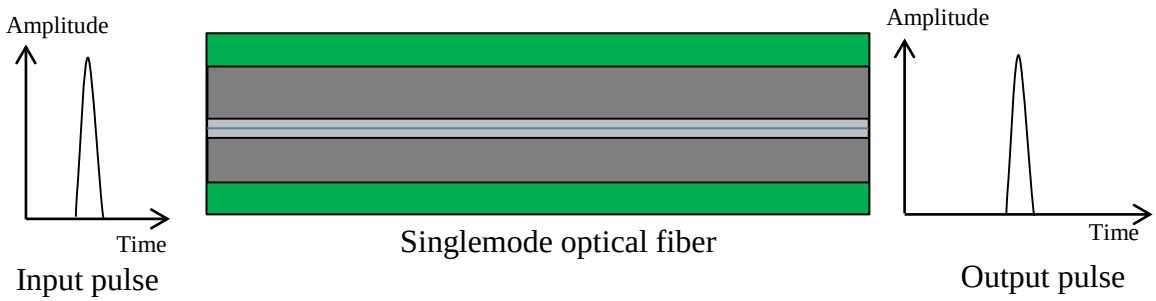

Figure 3.4. *Propagation of light in a singlemode optical fiber.*

Although, the light propagates through the fiber by means of total internal reflection, which ideally would suggest zero losses, some of the optical power is lost due to absorption in the impurities of the core and cladding, scattering from non-uniformities, and fiber bend loss. Typical losses for a single-mode fiber is in the order 0.25…0.4 dB/km.[13]

3.3 Laser

Laser ("light amplification by stimulated emission of radiation") is a source of light that produces coherent and nearly monochromatic light [14]. The physical phenomenon of the laser's operation can be examined with photons and atoms.

If an atom has an excited energy level E_a above ground level, it can absorb a photon with a wavelength λ_0 given by

$$E_a = hf_0 = \frac{hc}{\lambda_0}, \tag{3.5}$$

where f is the frequency, c is the speed of light, and h the Plack's constant [15, p.177]. When the energy of the excited atom falls back to the ground level, a photon is emitted. The emitted photon has the same wavelength as the one that was previously absorbed. However, the phase and direction of the emitted photon are random. This process is called spontaneous emission and is depicted in Figure 3.5.

Lasers utilize a phenomenon called stimulated emission, which is presented in Figure 3.6.

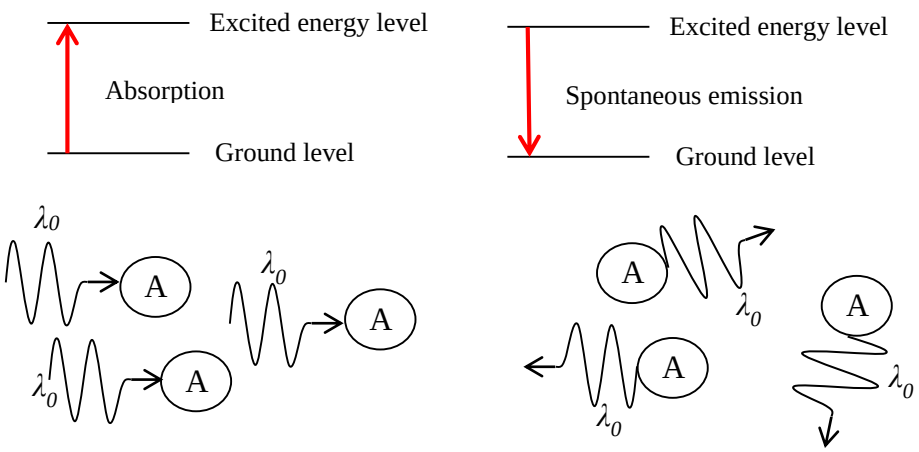

Figure 3.5. *Spontaneous emission of photons.*

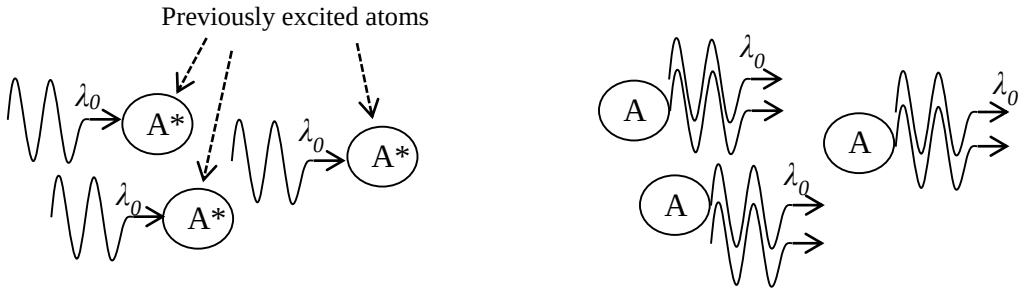

Figure 3.6. *Stimulated emission of photons.*

In stimulated emission, photons encounter an atom that has been previously excited. As a result, a resonance effect stimulates the atom to emit a photon with the same direction, wavelength, polarization and phase as the incident photon, thus producing coherent radiation. For each atom, there is one photon before and two photons after the stimulated emission, giving rise to light amplification. [10, p.1467]

3.3.1 Semiconductor laser

Upstream lasers used in HFC and RFoG networks are semiconductor lasers and are built from three elements: a laser cavity, a pump, and a mirror system, as presented in Figure 3.7.

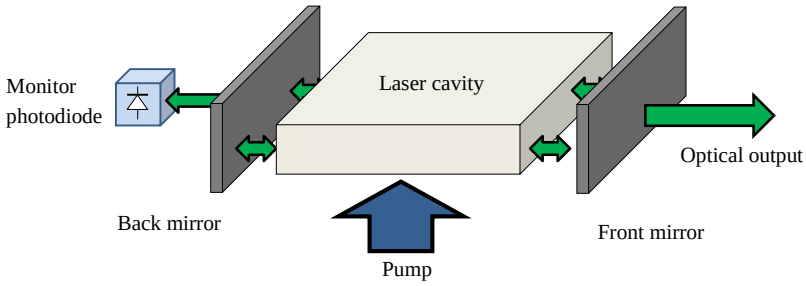

Figure 3.7. *Depiction of the elements in a semiconductor laser. Adopted from [6, p.143].*

The pump is an external energy source that provides the energy that is coupled to the laser and used to excite the atoms. In semiconductor lasers, the energy is delivered to the laser cavity with an electric current [12, p.432]. With the aid of the front and back mirrors, photons are reflecting in the laser cavity and coherent light is formed by stimulated emission. Some of the incident light will pass the front mirror and is lensed into an optical fiber.

There will be a set of optical wavelengths that can propagate through the cavity without being severely attenuated. These wavelengths, for which the optical beams of light behave as standing waves, depend on the cavity dimensions and optical characteristics. An example of the allowed wavelengths is presented in Figure 3.8.

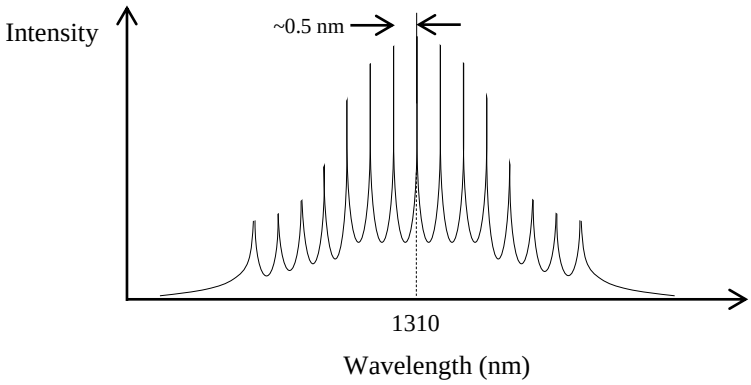

Figure 3.8. *Allowed wavelengths in a Fabry-Perot laser.*

A Fabry-Perot is a laser, whose optical output consists of many wavelengths around the center wavelength. Light can propagate through the cavity at all allowed wavelengths, but the light amplification is greatest in the center frequency.

By periodically modifying the optical characteristics of the cavity, wavelengths other than the center can be suppressed. This technique, known as grating, acts as an optical filter, and causes wavelengths around the center to be attenuated for more than 50 dB. This type of a laser is called distributed feedback (DFB) laser.[6, p.145]

As depicted earlier in Figure 3.7, laser modules used in optical communications include a photodiode, which is often utilized in a closed loop power control circuit. The monitor photodiode is usually connected in the control circuit in reverse bias, meaning its cathode is connected to a higher potential compared to the anode. The photodiode allows current to flow from its cathode to anode, if the laser transmits light. The magnitude of the photodiode current is proportional to the transmitted optical power. Thus, the photodiode is a crucial, but a rather simple component in a laser power control circuit. It can be used to sense the output power of the laser by measuring its current.

Figure 3.9 presents an example of a laser diode used in RFoG micronodes.

Figure 3.9. *A 1310 nm semiconductor laser.*

The package includes pins for the laser diode and the monitor photodiode. In addition, a singlemode optical fiber with a square connector (SC) is integrated to the package.

3.3.2 Optical modulation index

Lasers can be modulated either directly or externally. Both schemes are presented in Figure 3.10. In external modulation, the light is modulated after it is emitted from the laser. The laser produces a constant optical output power and an external modulator is used to modulate the light by varying the amount of power it lets through. However, the external modulators are often bulky and expensive. In direct modulation, the optical power of the laser is modulated with the input current. Thus, an external modulator is not required. [16]

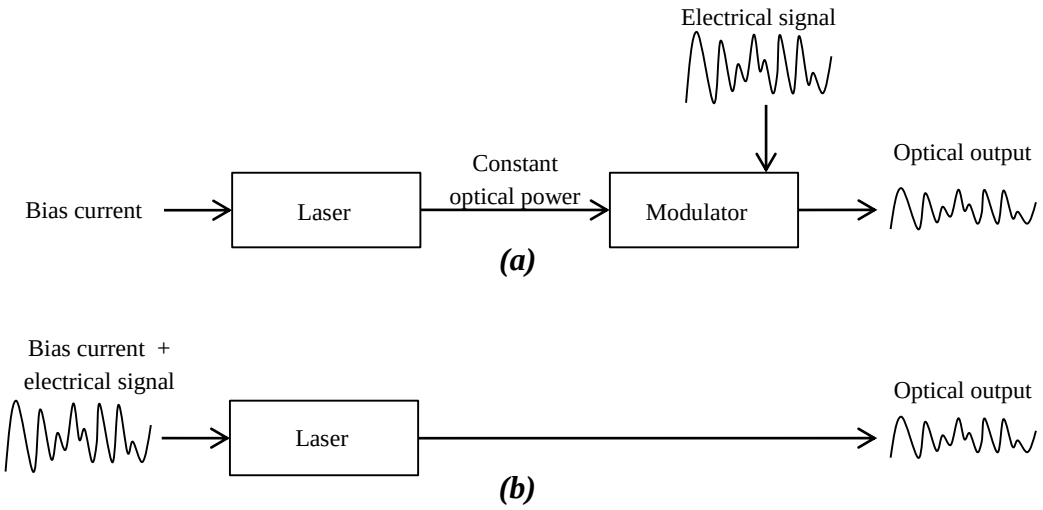

Figure 3.10. *(a) External and (b) direct modulation of a semiconductor laser.*

Semiconductor lasers used in RFoG micronodes are modulated using direct modulation, because it is more cost effective and requires less space. In direct modulation, the modulating RF current is applied to the same terminals (laser diode anode and cathode) as the bias current. This is presented in Figure 3.11.

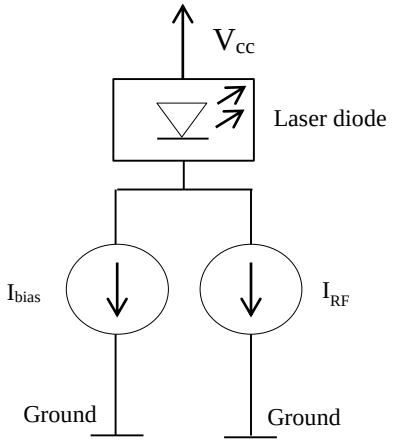

Figure 3.11. *Direct modulation of a semiconductor laser.*

The bias current sets an operating point for the optical power. When the RF current is superimposed on the DC bias, the output power of the laser is modulated. Figure 3.12 presents an example of semiconductor lasers transfer curve. The transfer curve depicts the relation between the input current and the optical output power.

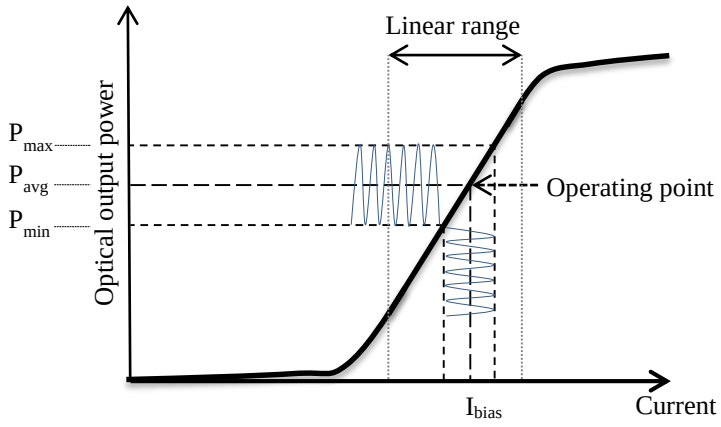

Figure 3.12. *The transmitted optical power of a semiconductor laser as a function of current.*

The laser is operated at a certain operating point in its linear range. The RF current, with minimum and maximum values of I_{min} and I_{max}, respectively, is superimposed on the bias current, thus modulating the intensity of the optical power. A quantity called optical modulation index (OMI) is used to measure the effect of the modulation signal to the light output. OMI can be defined as

$$OMI = \frac{P_{max} - P_{min}}{2P_{avg}}, \tag{3.6}$$

where P_{max} is the maximum optical power, P_{min} the minimum optical power, and P_{avg} the average power that occurs if only the bias is applied. [6, p.146]

As discussed in Chapter 2.2.1, the upstream laser of a micronode is switched on only if an upstream signal is present at the input. Hence, when there is no signal to be transmitted, the carrier light is switched off. This suggests that for a directly modulated micronode laser, the bias current is switched on and off depending on the RF input.

3.3.3 Thermal considerations

Micronodes are usually specified to operate in ambient temperatures from -40 to 85°C. It would be possible to cool (or warm) the lasers using thermoelectric coolers (TEC) to keep the operating temperature constant. However, they require considerable power and additional control circuitry, which makes them less attractive for a micronode product.

Concerns rise from the varying ambient temperature: the transfer curve and the RF output level may change and noise may increase. Semiconductor lasers are typically less efficient at higher temperatures. Thus, the linear range of the transfer curve is less steep, which in turn will lower the OMI and change the bias current for the specified average optical power. [6, p.156]

Changes in temperature also lead to tracking error. The monitor photodiode used to measure the optical power may give false readings as temperature changes. The tracking error can change in an undetermined way. Because the photodiode is usually part of an optical power control circuit, changes in its characteristics lead to varying optical power propagating in the fiber as temperature changes. [6, p.157]

3.4 Negative feedback and the operational amplifier

The laser bias, which sets the average output power, can be controlled by means of negative feedback. The basic structure of a negative feedback loop is shown in Figure 3.13.

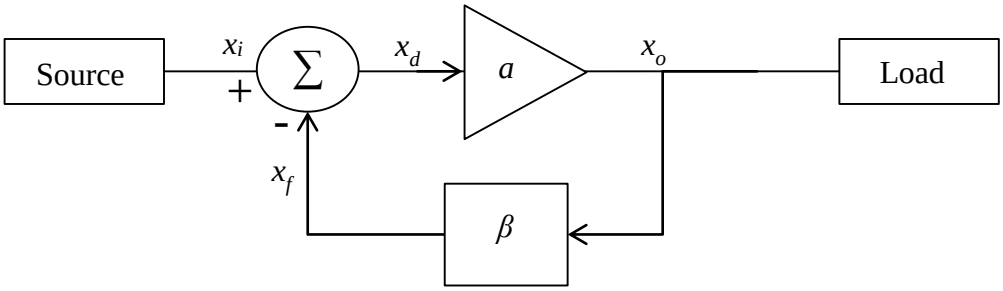

Figure 3.13. *Negative feedback loop.*

The symbol x stands for voltage or current, a the gain of the error amplifier (or open-loop-gain of the circuit), β gain (or feedback factor) of the feedback circuit.

The error amplifier amplifies its input signal x_d and produces an output signal $x_o = ax_d$. The feedback network takes a sample of the output x_o and produces a feedback signal $x_f = \beta x_o$. Now, the summing network $\sum$ generates the error signal $x_d = x_i - x_f$. Thus, the name negative feedback: a sample of the output is fed back to the input, where it is subtracted from the input signal.

The closed loop gain A of the circuit presented in Figure 3.13 can be expressed as

$$A = \frac{x_o}{x_i} = \frac{a}{1+a\beta}. \tag{3.7}$$

If the open loop gain a approaches infinity, equation (3.7) can be rewritten as

$$A_{ideal} = \lim_{a\to\infty} \frac{a}{1+a\beta} = \frac{1}{\beta}. \tag{3.8}$$

Now that $a >> \beta$, the closed loop gain A becomes independent of a. Thus, the closed loop gain is characterized only by the feedback network.

In electronics, control systems utilizing negative feedback is often realized with operational amplifiers. The operational amplifier (abbreviated as op amp) is a voltage amplifier with an extreme open loop gain a. For example, the popular 741 op amp exhibits a

typical open loop gain of 200 V/mV [17]. The symbol and equivalent circuit of an op amp is presented in Figure 3.14.

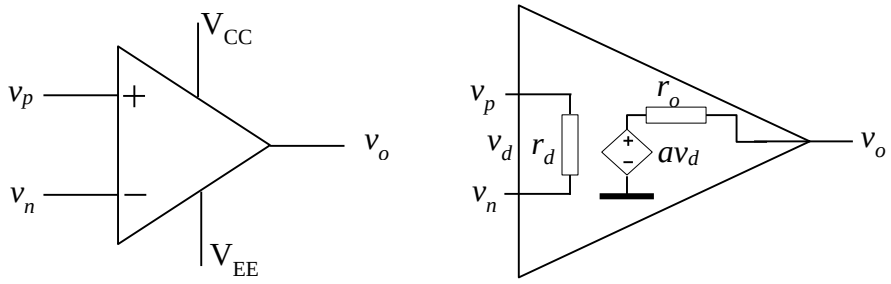

Figure 3.14. *Schematic symbol of an operational amplifier (left) and its electrical equivalent circuit (right.)*

The operational amplifier inputs, which are usually identified with symbols "+" and "-", are called the non-inverting and inverting inputs, respectively.

An operational amplifier amplifies the voltage difference between the non-inverting and inverting inputs. Therefore, the operational amplifier is a difference amplifier. The output of an operational amplifier can be expressed as

$$v_o = a(v_p - v_n) = av_d, \tag{3.9}$$

where a is the open loop gain, v_d is the differential input voltage, v_p and v_n the input voltages of the non-inverting and inverting inputs, respectively. An ideal operational amplifier has the following properties

$$a = \infty, \tag{3.10}$$

$$r_d = \infty, \tag{3.11}$$

$$r_o = 0, \tag{3.12}$$

$$i_p = i_n = 0, \tag{3.13}$$

where r_d is the differential input resistance, r_o output resistance, and i_p and i_n the input currents of the non-inverting and inverting inputs, respectively [18, p.7]. In real op amps, these values are naturally finite. For example, the inputs require a small input bias current. For example, a typical input current for an LM741 amplifier is 80 nA. [17]

When an operational amplifier is used as a part of a control circuit, it is equipped with negative feedback. A simple op amp circuit with negative feedback is presented in Figure 3.15. The circuit is known as a non-inverting amplifier.

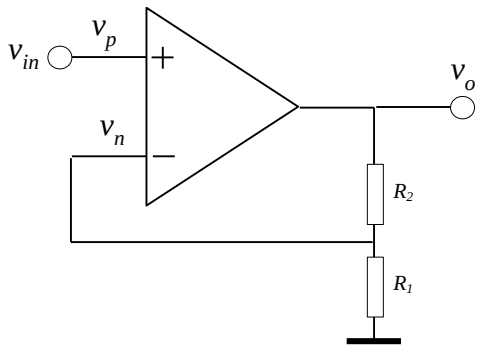

Figure 3.15. *A negative feedback, non-inverting operational amplifier circuit.*

The input voltages present in the above circuit can be written as

$$v_n = \frac{R_1}{R_1+R_2} v_o, \text{ and} \tag{3.14}$$

$$v_p = v_{in} . \tag{3.15}$$

Equation (3.9) can now be rewritten as

$$v_o = a(v_p - v_n) = a(v_{in} - \frac{1}{1+\frac{R_2}{R_1}} v_o). \tag{3.16}$$

The closed loop gain *G* of the circuit can now be expressed as

$$G = \frac{v_o}{v_{in}} = \left(1 + \frac{R_2}{R_1}\right)\left(\frac{1}{1+\frac{1+\frac{R_2}{R_1}}{a}}\right). \text{[18,p.9]} \tag{3.17}$$

Letting the open loop gain *a* (the gain of the operational amplifier) approach infinity, the closed loop gain G is reduced to

$$G_{ideal} = \lim_{a\to\infty} G = 1 + \frac{R_2}{R_1} . \tag{3.18}$$

The closed loop gain G_{ideal} of equation (3.18) represents an ideal situation where *a* is assumed to be infinite. A real op amp exhibits a large, but not infinite open loop gain. However, the assumption exploited in equation (3.18) can often be justified. For example, letting $R_2 = 3R_1$ and a = 200 V/mV = 200 000, the closed loop gains obtained from equations (3.17) and (3.18) are 3.999 and 4, respectively. The analysis proves that the closed loop gain of a negative feedback op amp circuit is primarily dominated by the feedback factor.

The operation of the circuit shown in Figure 3.15 can be expressed in a simple way: the negative feedback tries to adjust the voltage v_n to equal v_p by controlling the output

voltage v_o. Thus, by utilizing sensors and actuators, negative feedback can be utilized to control a physical quantity, such as the intensity of light transmitted by a laser.

3.5 Voltage comparator

A voltage comparator compares the voltages of its two inputs, the inverting and non-inverting, and outputs a digital signal indicating which one is larger. Therefore, a comparator can be considered as a 1-bit analog-to-digital converter.

An operational amplifier can be used as a voltage comparator. This is achieved by removing the negative feedback. Hence, the gain of the op amp circuit is only characterized by the large open-loop gain. The output voltage v_o of a voltage comparator is

$$v_o = V_{OL} \approx V_{EE}, \quad for\ v_p < v_n \text{ , or} \tag{3.19}$$

$$v_o = V_{OH} \approx V_{CC}, \quad for\ v_p > v_n, \tag{3.20}$$

where V_{EE} is the voltage of the lower supply and V_{CC} voltage of the higher supply. The comparator output as a function of input is illustrated in Figure 3.16. Figure 3.16 assumes a dual supply operation.

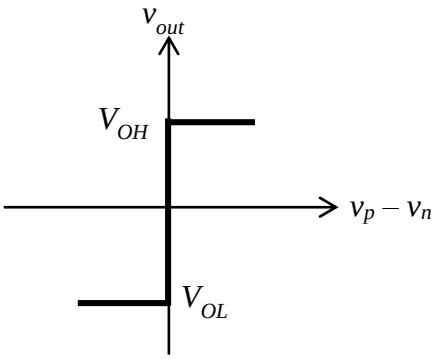

Figure 3.16. *Output characteristics of a dual supply voltage comparator.*

Especially in high-speed applications, the voltage comparator should be able to quickly switch the output voltage when the sign of $v_p - v_n$ changes. This is characterized by response time (also known as propagation delay). It is defined as the time it takes for the comparator to reach 50% of the output transition from the instant that the sign of $v_p - v_n$ changes. [18, pp.399-400]

Using an operational amplifier as a comparator in a high-speed application is a rather poor decision, because they are not typically able to reach fast response times. Op amps are designed to be operated in a closed-loop rather than open-loop configuration. The transistors used in op amp output stages are not switching transistors. Instead, they are designed to be highly linear. When these output transistors are saturated, it can take them several hundreds of microseconds (or even milliseconds) to recover. This leads to

long response times, when the op amp is configured to operate as a comparator. In addition, some op amps used in an open-loop configuration can consume considerably more power than expected. This is because the output is driven to the supply rail voltages. [19]

When speed is critical, general purpose comparators should be used instead of operational amplifiers. Comparators are designed to operate in open-loop configuration. Comparators often use a CMOS (Complementary Metal Oxide Semiconductor) output or an open-collector output. The main difference between the push-pull type CMOS and the open-collector output is that the latter needs to be loaded with an external pull-up resistor. An open collector comparator is presented in Figure 3.17.

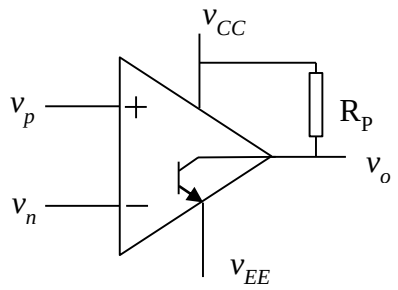

Figure 3.17. *An open-collector voltage comparator with an external pull-up resistor.*

The open collector comparator loaded with a pull-up resistor operates as presented earlier in equations (3.19) and (3.20). If $vp < vn$, the output stage transistor conducts, thus pulling v_o to the voltage V_{EE} (or ground, if single supply operation is used). However, if $vp > vn$, the output stage transistor will not conduct, and the output is pulled up to V_{CC} by the pull-up resistor R_p. General purpose comparator ICs achieve greater response times than operational amplifiers in comparator configuration. For example, response time for an LM292 comparator is 1.3 µs and 300ns with sufficient input overdrive [20], while a highspeed LT1720 can achieve a response time of 4.5 ns [21].

3.5.1 Response time and input overdrive

As discussed earlier, response time is defined as the time it takes the comparator to accomplish 50 % of its output transition, when the $v_p - v_n$ changes its sign [18, pp.399-400]. A depiction of response time for a non-inverting, single supply comparator is shown in Figure 3.18.

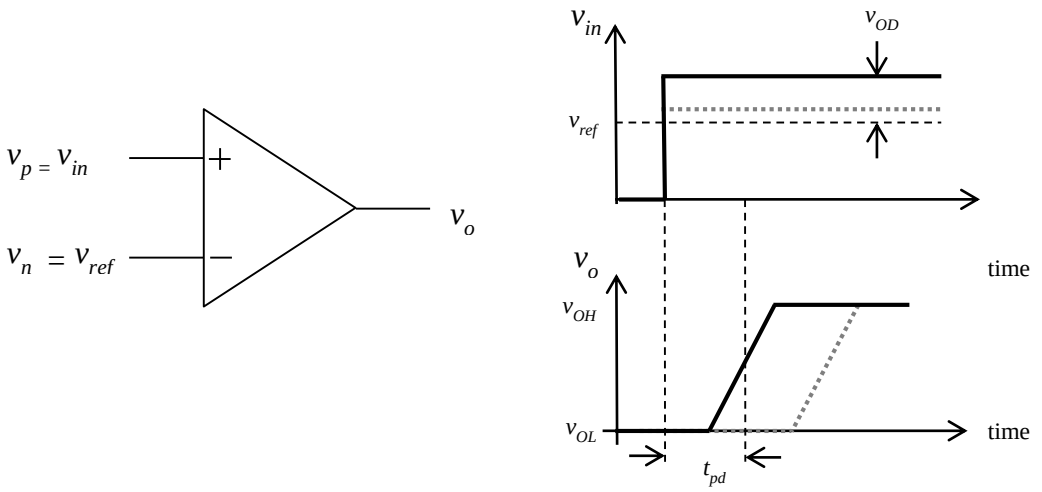

Figure 3.18. *Depiction of response time for a non-inverting comparator with two different values of input overdrive.*

The excess voltage v_{in} - v_{ref} is called the input overdrive voltage. As presented in Figure 3.18, greater input overdrive will result to smaller propagation delays [22].

3.5.2 Hysteresis

A comparator circuit can be externally modified to exhibit hysteresis. A single supply open-collector comparator with a hysteresis circuit and the hysteresis behavior is shown in Figure 3.19.

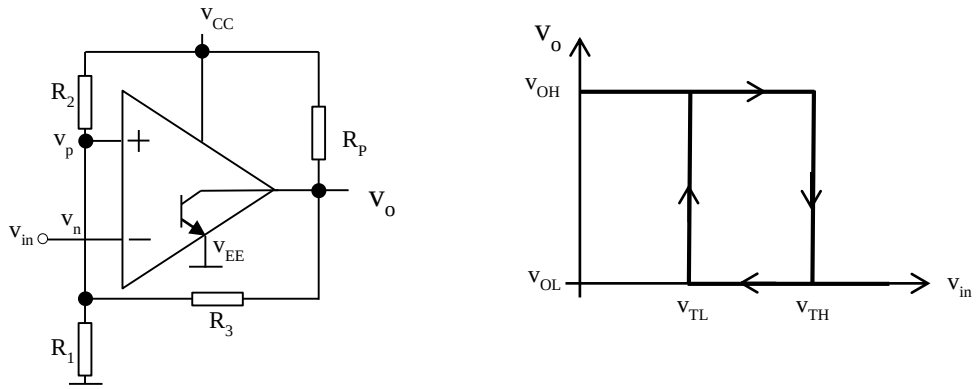

Figure 3.19. *A single supply comparator with hysteresis.*

The circuit above is often called a Schmitt trigger. When hysteresis is utilized, the output will change with different input voltages, depending if the output transition is from V_{OL} to V_{OH} or from V_{OH} to V_{OL}. Hysteresis is usually deployed to prevent voltage fluctuations in the input, caused by noise or other disturbances, to generate unwanted switching between the two output states. This is called comparator chatter. Figure 3.20 presents the behavior of a comparator with and without hysteresis.

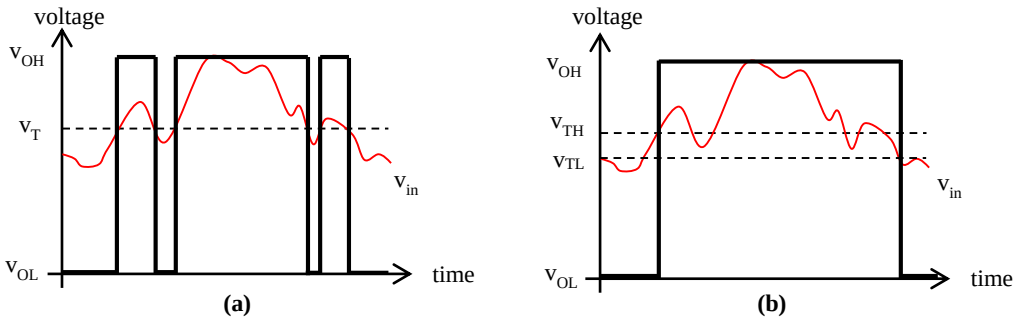

Figure 3.20. *Input vs output of comparator (a) without (b) with hysteresis. Output chatter is present in (a), but absent in (b).*

As presented in Figure 3.20, the presence of hysteresis is effective against output chatter, which occurs in Figure 3.20a, but not in 3.20b. Referring to the circuit in Figure 3.19, the input threshold voltages can be written as (assuming $R_p << R_3 + (R_1 \,||\, R_2)$ and a full rail-to-rail output swing)

$$V_{TL} = \frac{R_1||R_3}{(R_1||R_3)+R_2}V_{CC}, \qquad V_{TH} = \frac{R_1}{R_1+(R_2||R_3)}V_{CC} \text{ [18, p.419].} \qquad (3.21)$$

As seen from the equations above, the desired threshold voltages can be set by selecting appropriate resistor values.

3.6 RF detector

RF detectors are generally used for measuring RF power levels. For example, RF detectors can be used in transmitter and receiver designs. They can be used to measure the transmitted and received signal power, and utilized in transmit and receive power control, as depicted in Figure 3.21.

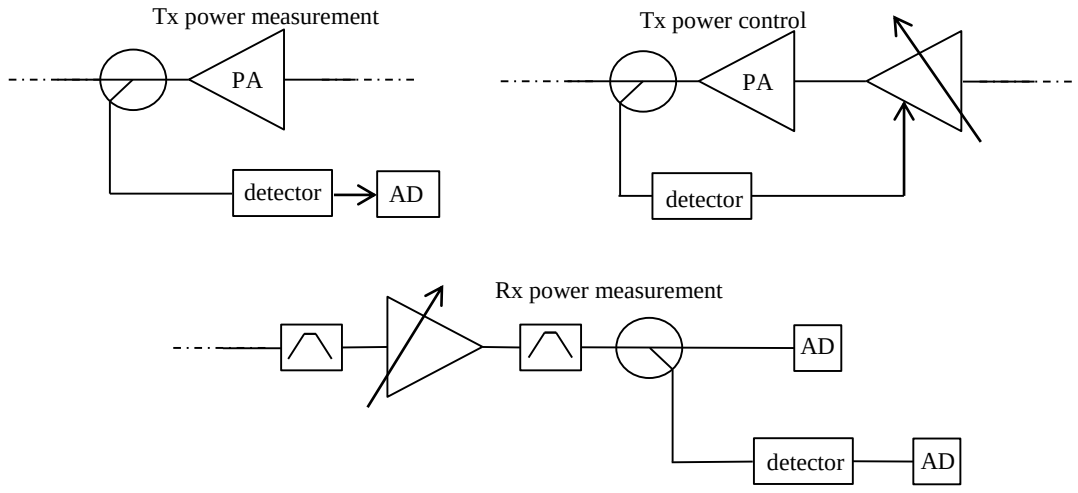

Figure 3.21. *Examples of RF detection applications.*

An RFoG micronode upstream transmitter spends most of its time in sleep-mode. It must be able to detect the incoming RF signal, and make the decision when to turn on for transmit. This is achieved by sensing the RF power in the coaxial input of the micronode, and deciding, whether it is high enough to be an actual signal. The detector is also used to sense when the input RF signal decreases below a certain threshold. When this lower threshold is crossed, the transmitting laser is switched off. The turn-on/turn-off power specifications for an RFoG micronode are given in Table 3.1.

Table 3.1. *Turn-on/turn-off specifications for an R-ONU [4].*

Specification	Value
Power range at which the micronode laser should turn on	67 – 76 dBuV
Power range at which micronode laser should turn off	52 – 61 dBuV

An RF detector monitors its input and produces a DC voltage proportional to the applied RF power. There are two basic types of RF detectors: the logarithmic (log) and the root-mean-square (RMS) type. The log type produces an output voltage linearly proportional to the logarithm of the input (dB value), whereas the RMS type produces an output linearly proportional to the RMS value of the signal.

The logarithmic detector (also called demodulating logarithmic amplifier, log amp) is usually chosen for applications which operate in burst mode, because they exhibit fast response times. An RMS detector is generally used in applications, where the signals of interest exhibit high (or widely varying) crest factor (peak-amplitude-to-RMS-power-ratio) [23]. The RF signal fed to a micronode upstream transmitter is OFDM N-QAM (N = 16, 32, 64, …, 4096) modulated signal for DOCSIS 3.1 (Data Over Cable Service Interface Specification). This would call for an RMS detector due to the high crest factor. However, the signal is operated in burst mode and RMS detectors are generally slow. They exhibit slow output DC voltage rise and fall times, which makes them unsuitable for the rather fast operation of an RFoG micronode. Therefore, the logarithmic type is more suitable.

Detector circuits can also be implemented using the nonlinear V-I relationship of a diode. However, a normal pn junction diode typically exhibits large junction capacitance. Thus, it is unsuitable for high frequency applications. In high frequency applications, a Schottky diode can be used instead. It utilizes a semiconductor-metal junction resulting in a lowered junction capacitance [24, p.527]. An example of a detector utilizing Schottky diodes and a difference amplifier is presented in Figure 3.22.

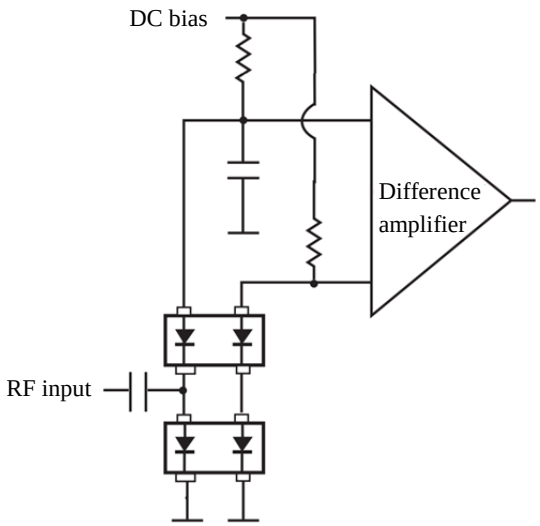

Figure 3.22 *A Schottky diode based RF detector. Adopted from [25].*

When RF is applied, a voltage difference is generated between the inputs of the difference amplifier. The difference amplifier amplifies this voltage and a DC voltage representing the detected RF power is obtained.

3.7 Impedance matching

Impedance matching is considered an important aspect in RF engineering. A perfect impedance match ensures that all of the available power is delivered and dissipated in the load. A perfect impedance match between a load and a source occurs when the output impedance of the source is the complex conjugate of the load

$$\begin{cases} \mathrm{Re}\{Z_L\} = \mathrm{Re}\{Z_S\} \\ \mathrm{Im}\{Z_L\} = -\mathrm{Im}\{Z_S\} \end{cases}, \tag{3.22}$$

where Z_S is the source impedance and Z_L load impedance [24, p.78]. Usually, the respective source and load impedances do not match at the initial situation. Therefore, a matching network needs to be implemented, as shown in Figure 3.23.

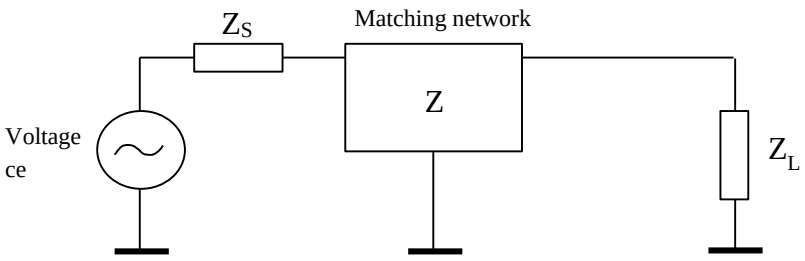

Figure 3.23. *A Matching network inserted between a load and a source.*

The matching network will transform the impedance seen by the source to the complex conjugate of its own impedance, and therefore, enable maximum power transfer. Match-

ing network is usually constructed from reactive components to achieve (ideally) a lossless match. A matching network can be implemented with lumped components (inductors, capacitors, and resistors) or with transmission line elements such as open-ended or shorted transmission line stubs.

It is crucial that the input of an RF detector is impedance matched to its source. If the impedance of the detector input is not matched with the source, all of the available power is not delivered to the detector. This will lower the sensitivity of the detector circuit.

In addition, a detector may be required to operate in a wide bandwidth. For example, an upstream power detector used in a DOCSIS 3.1 RFoG system needs to be able to detect powers in a band of 5 – 204 MHz. Therefore, the detector input must be matched in the whole band. If there is an impedance mismatch at some parts of the band of interest, the detector may give false readings of the detected power in those frequencies. This is because some of the available power is reflected back to the source, and not delivered in the detector.

4. RFOG MICRONODE LASER DRIVER DESIGN

The objective of this thesis is to design and implement a bias control circuit for a micronode transmitter, which could be realized in a Teleste corporations future RFoG product. This chapter presents the components and designed electronic architectures that were considered for the device.

The proposed design for the upstream transmitters laser driver circuit consists of 3 blocks: the RF detector, the voltage comparator and the laser bias control circuitry. The RF detector and the voltage comparator are used to sense whether or not a signal is present at the coaxial input of the device. The laser current control circuit is used to switch on and off the transmitting laser and keep its bias current regulated. These blocks can be realized using integrated circuits (ICs) or discrete components. For example, the RF detector can be designed using Schottky diodes or a detector IC, such as a logarithmic detector.

The realized device must meet the requirements presented in Table 4.1.

Table 4.1. *Requirements for an RFoG upstream transmitter according to SCTE RFoG specification [4].*

Specification	Requirement
Input RF power at which the transmitting laser should turn on	67 - 76 dBuV
Input RF power at which the transmitting laser should turn off	52 - 61 dBuV
Maximum time delay from application of RF to optical power rising to 90% of its steady state amplitude	1.3 µs
Minimum 10 – 90 % optical power rise time	100 ns
Maximum 10 – 90 % optical power rise time	1 µs
Maximum time delay from removal of RF to the time optical power falling to 10 % of its steady-state amplitude	1.6 µs
Maximum 90 – 10 % optical power fall time	1 µs
Minimum 90 – 10 % optical power fall time	100 ns

4.1 Block diagram and the principle of operation

Figure 4.1 presents a block diagram that could be utilized as an RFoG micronode upstream transmitter and acts as a basis for this thesis. The red line encloses the scope of this thesis.

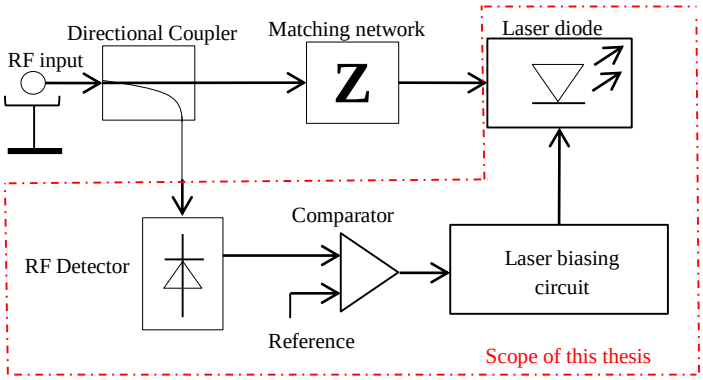

Figure 4.1. *Micronode upstream transmitter block diagram.*

In the above block diagram, RF is fed into a directional coupler, which couples a portion of the RF signal to the detector circuitry. The detector converts RF power to DC voltage. The detector is followed by a voltage comparator, which makes the decision if the laser should be turned on (or turned off). The comparator must exhibit a hysteresis behavior, because the thresholds of laser turn-on and turn-on powers differ, as presented earlier in Table 4.1.

The output of the comparator is connected to the bias current control circuitry. If the detected signal power exceeds the turn-on threshold, the comparator will signal the bias control circuitry to drive a regulated bias current through the laser diode. Furthermore, when the RF power decreases below the turn-off threshold, the bias current is switched off and the laser is shut down.

The main portion of RF going through the coupler is fed to the laser through a matching circuit. The circuit will transfer the impedance seen in the RF input from the low impedance value of the laser to the 75 Ω characteristic impedance used in cable systems in order to achieve maximum power transfer as discussed in Chapter 3.7. The matching circuit must be relatively broadband: the upstream bandwidth in a DOCSIS 3.1 system can be 5 – 204 MHz at maximum. However, the development of the modulation circuit and laser modulation is not included in the scope of this thesis: only the mechanism for laser turn-on and turn-off is designed.

4.2 Upstream signal detection

The SCTE RFoG specification dictates the turn-on and turn-off input powers. The laser must turn on, when the input power reaches the range from 67 dBuV to 76 dBuV, and must turn off when the input power decreases to the range of 52 dBuV to 61 dBuV. Thus, the detector circuitry can be thought to be composed from two components: the actual detector as well as the comparator. The turn-on and turn-off input power regions are depicted in Figure 4.2.

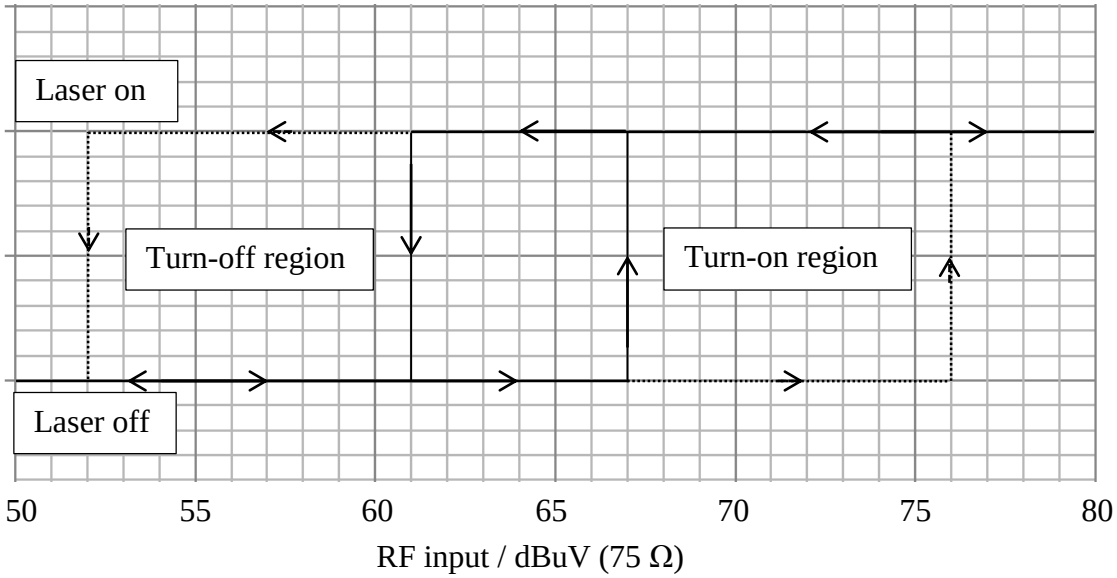

Figure 4.2. *Turn-on and turn-off input RF power regions of a micronode laser.*

As disclosed in the SCTE RFoG specification, the turn-on/turn-off characteristics of the device shall be measured with single carrier continuous wave. [4]

The home cable modem, which provides the upstream input signal for a micronode, can be assigned to any available transmit channel inside the upstream bandwidth. The upstream bandwidth can be as wide as 54 – 204 MHz for DOCSIS 3.1. Thus, the measured value of power cannot vary too much as a function of frequency. The detector must give as consistent measurement result as possible for any input signal in the upstream band. Figure 4.3 depicts the wanted and unwanted frequency characteristics of the detector.

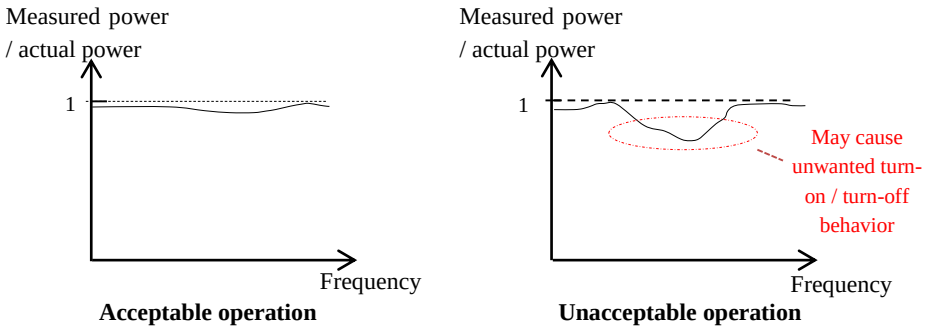

Figure 4.3. *An RF detector may give false readings if its input is not adequately well matched.*

As discussed in Chapter 3.7, unacceptable operation may occur, if the input impedance of the detector is not matched with its source in the whole upstream band. Some variation in the measured power is acceptable, due to the relatively wide threshold ranges that were presented in Figure 4.2. However, if the detector is not properly impedance matched in some range of the upstream bandwidth, problems may rise in form of non-uniform turn-on / turn-off operation.

The input of an RF detector cannot distinguish an unwanted signal from the signal of interest. For example, noise from 50 Hz (or 60 Hz) humming, spurious emissions from some other block of the device (e.g. clock, oscillator, etc) or emissions from nearby devices may be higher in power than our signal of interest at the lower end of the dynamic range. This can lead to high signal-to-noise ratio (SNR). Thus, careful shielding, grounding, and filtering is essential.

4.2.1 Detector

Three different detector circuits were chosen for testing and comparison: An AD8307 logarithmic detector [26], an LT5537 logarithmic detector [27], and a discrete solution utilizing Schottky diodes [25] with an MC33172 op amp [28]. The application circuits of the detectors are presented in Figure 4.4.

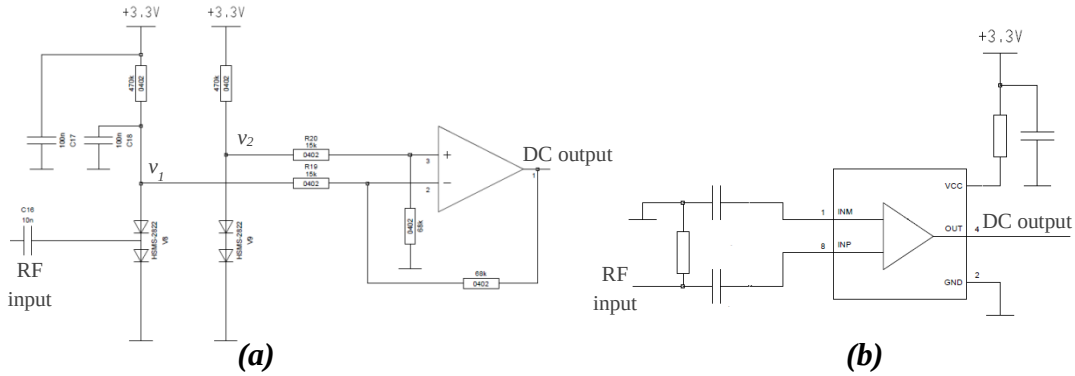

Figure 4.4. *a) A discrete detector design utilizing Schottky diodes and an operational amplifier b) An IC solution with either AD8307 or LT5537.*

The idea for the detector circuit of Figure 4.4a was obtained from the HSMS-282x Schottky diode datasheet [25]. The circuit is essentially a voltage doubler, whose output voltage is amplified using a difference amplifier. When RF is applied to the input, voltage v_1 decreases, and $v_2 - v_1$ will be a non-zero, positive voltage. The operational amplifier will then amplify this voltage difference. The operation of the circuit verified with LTSpice simulation software. In the case of Figure 4.4a, output voltage of the operational amplifier is

$$v_o = \frac{68\ k\Omega}{15\ k\Omega}(v_2 - v_1) = 4{,}533(v_2 - v_1)\ . \qquad (4.1)$$

Figure 4.4b presents the basic circuits for the chosen logarithmic amplifiers. The logarithmic detectors that were considered for the design were equipped with a shunt 75 Ω resistor in their inputs in order to achieve broadband impedance matching. 75 Ω is traditionally the characteristic impedance used in cable TV networks, rather than 50 Ω that is used in many other applications of RF engineering. The method of inserting a shunt 75 Ω resistor in the log amp inputs were suggested in the datasheets.

The datasheets report that the two logarithmic amplifiers exhibit similar RF-to-DC slopes: AD8307 a slope of 25 mV/dB and LT5537 a slope 20mV/dB. Furthermore, the slopes of both detectors are adjustable using an external resistor.

The operating range of the AD8307 is specified to be from DC to 500 MHz. The range of LT5537 is specified from 10 MHz to 1000 MHz, although the lower end can be extended by placing an external capacitor in the CAP+ and CAP- pins (not depicted in Figure 4.4) of the IC. A 33 nF external capacitor was found adequate.

Logarithmic detectors are usually AC coupled. Therefore, the positive and negative RF input pins should be preceded with coupling capacitors, as is presented in Figure 4.4. 100 pF coupling capacitors were used for both log amps. A terminating resistor is also

inserted between the high and low RF inputs. A typical input impedance of a logarithmic amplifier is typically in the range of kiloohms. Due to the fact that a logarithmic amplifier response to the input voltage rather than input power, the impedance matching between the source and the load can be achieved with a resistor of 75 Ω rather than with reactive components. It was found that the terminating resistor can be inserted either detector or source side of the coupling capacitors without a noticeable effect. They were ultimately placed in the source side of the log amps.

The measurement results for the detectors are presented in Chapter 5. The results were used for comparison and choosing the most suitable detector for the application.

4.2.2 Voltage comparator

The comparator is a rather essential component in the proposed design: it will make the decision when to turn-on and turn-off the laser. The output of an RF detector is a DC voltage. A voltage comparator is used to compare the output voltage of the detector to a reference voltage. Therefore, the combination of an RF detector and voltage comparator basically compares the input power to a reference power. Two different ways of connecting the detector and comparator is presented in Figure. 4.5.

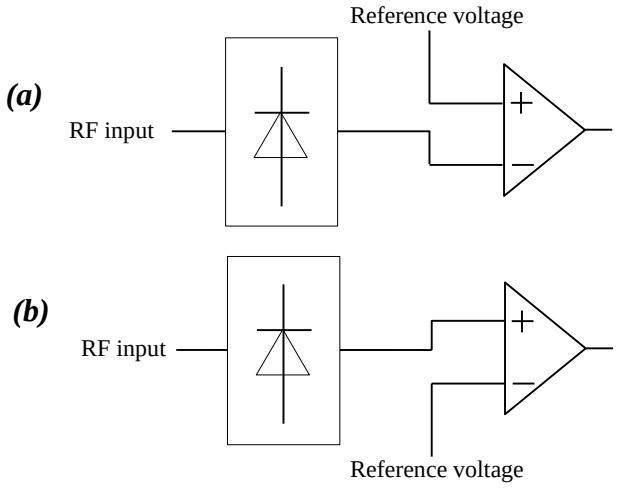

Figure 4.5. *Connecting the detector output to (a) inverting (b) non-inverting input of the comparator.*

In the proposed design, the detector output is connected to the inverting input of the comparator, and the reference voltage to the non-inverting input, as presented in Figure 4.5a. When the detector output voltage exceeds the reference voltage, the output voltage of the single supply comparator will be near 0 V (assuming single supply), as discussed in Chapter 3.5. On the other hand, when the detector voltage is lower than the reference voltage, the output of the comparator will be driven near the voltage of the positive power supply, for example 3.3 V.

Note that the detector-comparator-combination could also be connected in a way that the detector output would be connected to the non-inverting input, and the reference voltage to the inverting input (Figure 4.5b). In this case, the output voltage would be driven high when the detector output voltage exceeds the reference voltage, and driven low when the detector output voltage is lower than the reference. For some, this might be the more intuitive approach – a higher voltage given for high power and a low voltage given for low power. The option presented in Figure 4.5a was chosen because it supports the designed current control architecture, which is presented later in Chapter 4.3.2.

As presented in Table 4.1, the threshold powers for laser turn-on and turn-off do not equal. Therefore, the reference voltage at the non-inverting input of the comparator must be different depending on the state of the laser. When the laser is turned off, the reference voltage must be higher than when the laser is on. This is achieved by means of external hysteresis circuit, as discussed in Chapter 3.5.2. Without the hysteresis, the turn-on and turn-off powers would equal and the SCTE RFoG specification would not be met.

Two different voltage comparators were available for comparison: an open-collector output LM293D [20] and a CMOS output LT1720 [21]. The LT1720 was chosen for the final product because of its much faster response time. The datasheets state that with similar test conditions the response times for the LM293D and LT1720 are 1.3 µs and 7 ns, respectively. The specification for "maximum time from application of RF to optical power rising to 90% of its steady state amplitude" is 1.3 µs. Therefore, with the use of LM293D, this would be never achieved.

4.3 Bias current control

The output of the comparator will provide a logical input to the bias current control circuit. As discussed earlier, 0 V (logical 0) represents the presence of RF, whereas a 3.3 V (logical 1) represents absence of RF. The output of the comparator is connected to an analog single-pole-single-throw switch, which will control a mechanism that enables or disables current from flowing through the semiconductor laser.

The optical power of the laser is proportional to the current flowing through it. Therefore, the optical power can be set with a current regulator. However, it is crucial that the current regulator is able to switch on and off its current in order to meet the specifications of optical turn-on and turn on-times set by the SCTE RFoG specification [4]. The specifications for optical rise and fall times were presented in Table 4.1.

4.3.1 Current regulation

When the laser is supposed to be on, its bias current must be regulated. The current regulation circuit can be designed using an operational amplifier with negative feedback. There are two ways of realizing the feedback: the laser bias current can be sensed using a small, low tolerance resistor, or by utilizing the built-in photodiode. Although both techniques can be used, the method including the photodiode has one major advantage. As explained in Chapter 3.3.3, the transfer curve of the laser changes as a function of temperature. Thus, when the temperature changes the bias current to obtain a certain optical output needs to be adjusted. The feedback resistor cannot compensate on this change on its own. However, the photodiode produces a current through it that is proportional to the optical output power. Therefore, while the bias current to obtain a certain optical power changes as a function of temperature, the photodiode current versus optical output power remains almost constant. However, there is a small tracking error, but it is much lower than the error that would occur in the utilization of a feedback resistor.

The most challenging aspect of designing a current control scheme will be the turn-on and turn-off times presented earlier in Table 4.1. The turn-on and turn-off delay times of 1.3 µs and 1.6 µs, respectively, are relatively short. Therefore, response times occurring in the control circuitry, must be kept in minimum without risking the stability. A high slew rate of the current control circuitry might give rise to ringing and over-shooting, and a situation might occur, where a tradeoff between the rise time and settling time must be made.

An op amp MC33172D exhibiting a relatively low slew rate of 2.1 V/µs was chosen to serve as the current controlling component due to its instant availability and single supply operation [28]. A design for bias current control is presented in Figure 4.6.

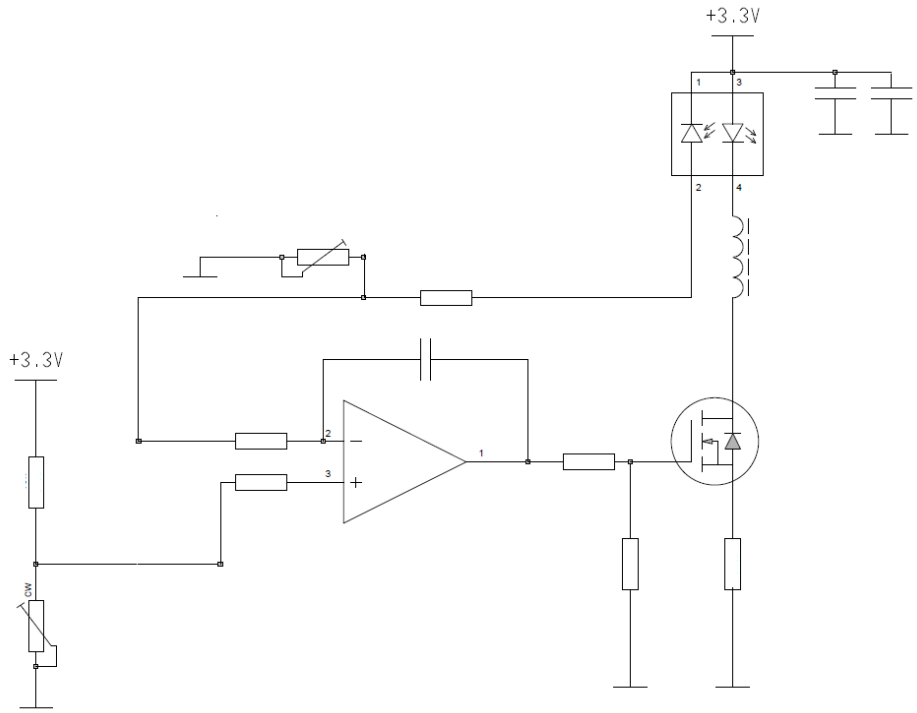

Figure 4.6. *A proposed current regulation control circuit.*

The most central component in the laser current control is the negative feedback operational amplifier supplying the gate of the MOSFET. Together they operate as a current regulator. As discussed earlier, there are two different methods to provide feedback for the operational amplifier. The feedback can be realized using the photodiode, which senses the output optical power, or a resistor sensing the laser current. For the design proposed in this thesis, the feedback utilizing the photodiode was chosen.

As discussed in Chapter 3.4, the operational amplifier loaded with negative feedback adjusts its output voltage to achieve a state, where the voltages at the inverting and non-inverting inputs equal. In the circuit of Figure 4.6 this is achieved as follows. The operational amplifier adjusts its output voltage to a value, where the photodiode passes a reverse (cathode-to-anode) current through it that leads to a voltage at the inverting input equaling the voltage at the non-inverting input. The block diagram in Figure 4.7 clarifies the mechanism how the optical power is regulated in the circuit.

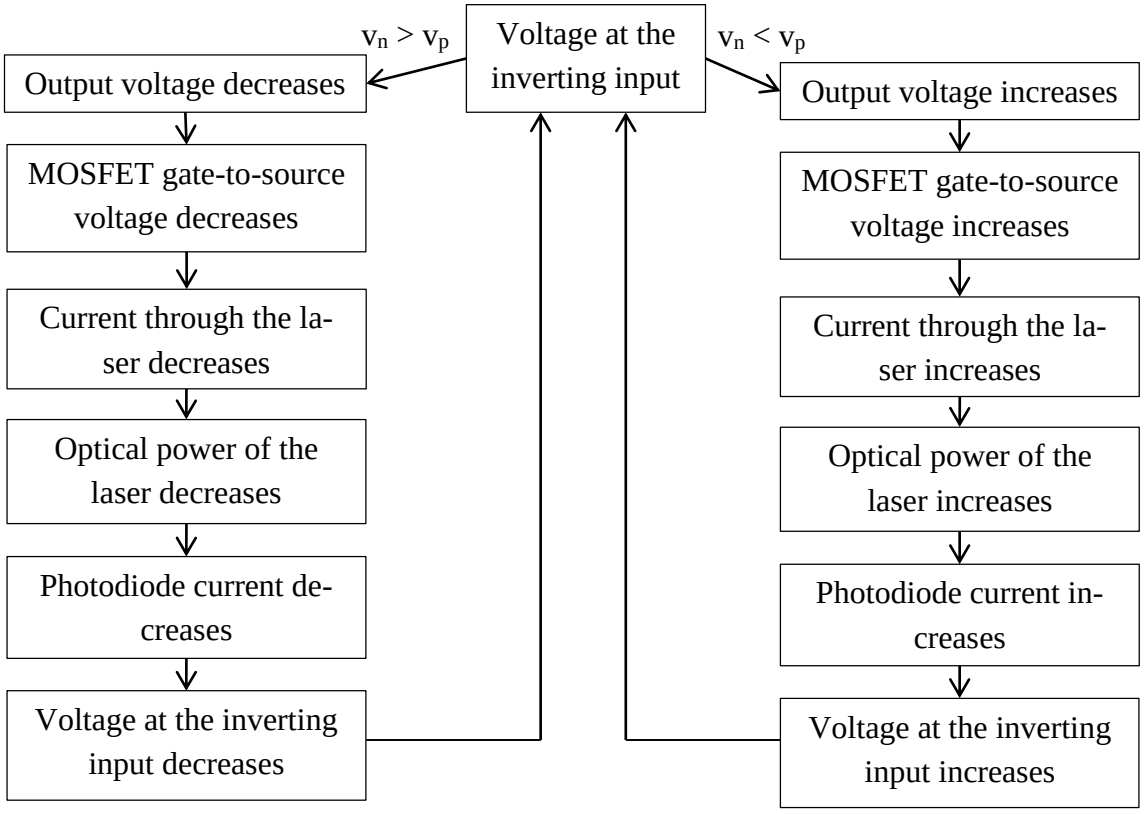

Figure 4.7. *Current regulation mechanism of the circuit proposed in Figure 4.6.*

Using a potentiometer, the voltage of the operational amplifiers non-inverting input can be adjusted. Thus, the steady-state output power can be adjusted. This can be used to fine tune the steady-state optical power to a desired value.

4.3.2 Current on/off switching

The laser is supposed to be on only when RF is sensed by the detector. Therefore, the bias current regulated through the laser must also be turned on and off. This is achieved by manipulating the voltage presented at the non-inverting input of the operational amplifier by utilizing a single-pole-single-throw analog switch. This is presented in Figure 4.8.

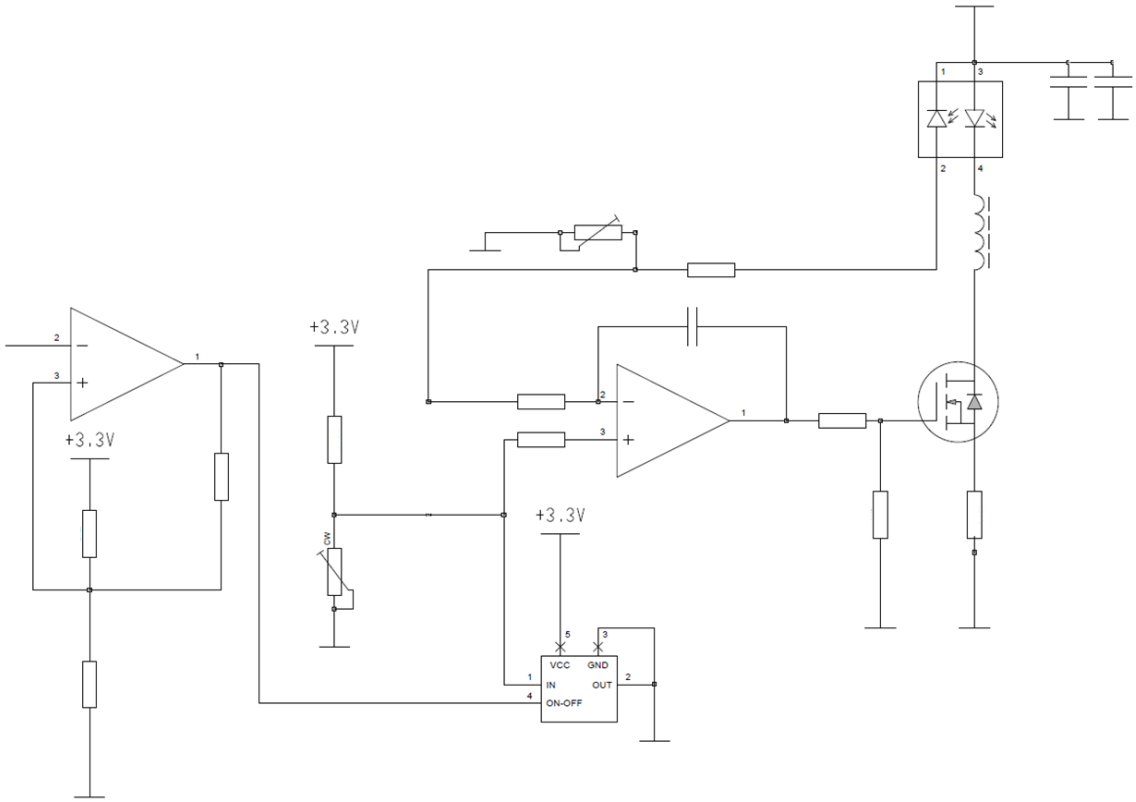

Figure 4.8. *Current regulation circuit with an added analog switch at the non-inverting input of the operational amplifier.*

The truth table for the analog switch is presented in Table 4.2.

Table 4.2. Truth table for the analog switch.

Input	Switch state
0	Open (does not conduct)
1	Closed (conducts)

First, the logical inputs, which are provided by the voltage comparator placed after the RF detector, shall be defined. The input of logical 1 (3.3 V) represents the absence of RF power presented to the detector, whereas a logical 0 (0 V) represents sufficient power at detector input.

When enough RF is present at the detector input, the voltage comparator will output 0 volts (logical 0). The switch will be open (not conducting), and current is regulated as discussed in Chapter 4.3.1. However, when enough RF is not applied, the output of the comparator will be 3.3 V (logical 1). The switch will now be closed (conducting) and the non-inverting input will be pulled down to ground. Again, the negative feedback of

the operational amplifier adjusts its output voltage in order to achieve a state, where the voltage at the inverting and non-inverting inputs equal. Consequently, the laser is shut down.

Other solutions for the on/off switching were also considered, but rejected after initial measurements. For example, one solution was to insert the analog switch in series the laser diode, rather than in the non-inverting input of the op amp. The on-off switching would have been achieved by closing and opening the path for the current to flow from the power supply to ground through the laser. The major drawback with this kind of a design is that when the switch is opened (no current will be able to flow through the laser), the output voltage of the operational amplifier would be driven to the positive rail. This is because the negative feedback would try to achieve a state, where the voltages of the inverting and non-inverting inputs would equal, although in this case it would be impossible. Now, at the time instant when the switch is closed, the voltage of the operational amplifier would be initially too high. In addition, the transistors in the output stage of the op amp would be saturated, requiring a long time to recover back to the linear range, as discussed in Chapter 3.5. The result is a substantial overshoot in the optical power before the regulation current achieves the steady state.

4.4 Construction of the prototype

A schematic and layout was designed using Mentor Graphics. The realized prototype included two types of RF detectors for separate use (selectable with a switch), a voltage comparator, and different current control circuits (selectable with a switch). The different methods for laser current control were implemented for comparison. The proposed design presented previously in Figure 4.8 was found to be the most suitable.

The prototype board also included DC-DC converters that were used to produce supply voltages for the components. The PCB was etched by a third party and the components were soldered at Teleste premises using reflow, wave, and manual soldering. The prototype is presented in Figure 4.9.

The prototype included a number of components that were not used in final the design. For example, the same PCB was used to test the solderability of components used in a different project.

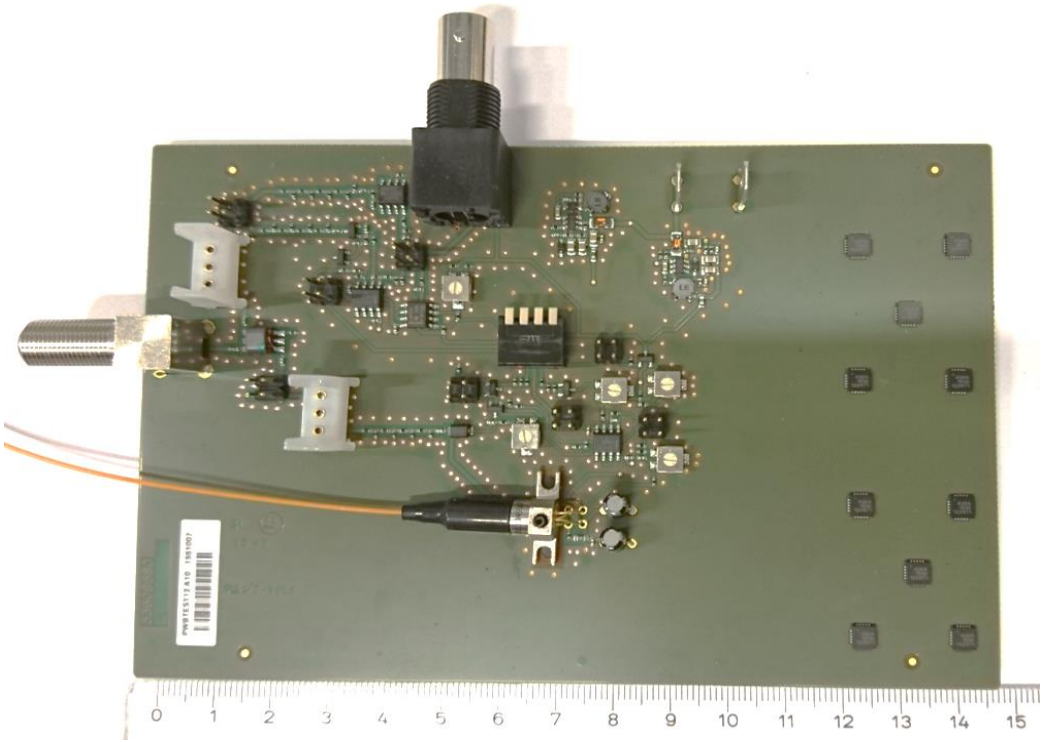

Figure 4.9. *Realized laser driver prototype.*

5. MEASUREMENTS

This chapter first presents the measurement results for different detectors that were considered for the design. The obtained results were used to choose the most suitable detector. Finally, the measurement results for the whole device are presented. Results are presented for the laser turn-on and turn-off input powers and response times. Furthermore, the measurement results are compared with the SCTE RFoG specification requirements.

5.1 Detector comparison

Three different detectors were compared. Two of them were located in the prototype board presented earlier in Figure 4.9 and one of them was measured in an external evaluation board. The properties of interest were the RF-to-DC conversion and response times. Great differences between the output rise/fall times and RF-to-DC conversion were found. Two of the measured detectors were logarithmic detector ICs and one was a discrete design. Table 5.1 summarizes the measured detectors.

Table 5.1. *Measured and evaluated RF detectors.*

Sample	Type	Component
Detector A	Logarithmic detector IC	LT5537
Detector B	Logarithmic detector IC	AD8307
Detector C	Discrete design utilizing Schottky diodes with an operational amplifier	Schottky diodes HSMS-2822 and op amp MC33172D

5.1.1 RF-to-DC transfer curve

The RF-to-DC transfer curve was measured for each of the three detectors in order to compare their performance. A suitable micronode RF detector should be able to exhibit a consistent operation in the whole 5 – 204 MHz upstream band: a given input power should lead to an approximately same output DC voltage in the whole bandwidth.

A 50 Ω RF signal generator was used to produce the input signal for the detector. A 50 Ω to 75 Ω matching pad, with an insertion loss of 4.0 dB, was placed between the gen-

erator output in order to obtain a 75 Ω test source. The detector output DC voltage was measured using a voltage meter. The RF input power was swept from 40 dBuV to 114 dBuV, with 2 dB power steps. The measurement frequencies were chosen to be 5, 100, and 204 MHz. A diagram of the measurement circuit used for measuring the RF-to-DC transfer curve of the detectors is presented in Figure 5.1.

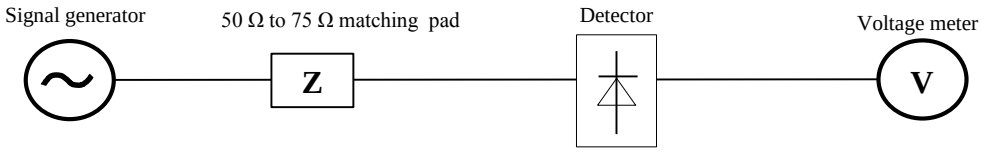

Figure 5.1. *Measurement circuit for different detectors.*

The measurement results for the RF-to-DC transfer curves for the detectors A, B, and C are shown in Figures 5.2 – 5.4, respectively.

For Detector A, the RF-DC transfer curve is linear. In addition, it remains relatively constant for the frequencies of 5, 100, 204 MHz. The variation of the transfer curve for different frequencies is especially low in the power range of 40 to 65 dBuV.

Detector B exhibits very similar behavior as Detector A. However, the output voltage for a given RF input is more frequency dependent in the whole input range of 40 to 114 dBuV. In addition, it is observed that the output starts to saturate with input powers greater than 100 dBuV.

Detector C has a relatively poor sensitivity: it can only detect input powers greater than 86 dBuV. In addition, the RF-to-DC transfer curve is exponential, as opposed to the linear behavior seen in Detectors A and B.

All of the measured detectors exhibited a good frequency behavior. Their RF-to-DC transfer curves remained relatively constant for different input signal frequencies. This suggests that the input impedances of the detectors are adequately broadband matched to the 75 Ω source. If there were too much of frequency dependent mismatch in the inputs, the RF-to-DC transfer curves would differ more noticeably for the different frequencies.

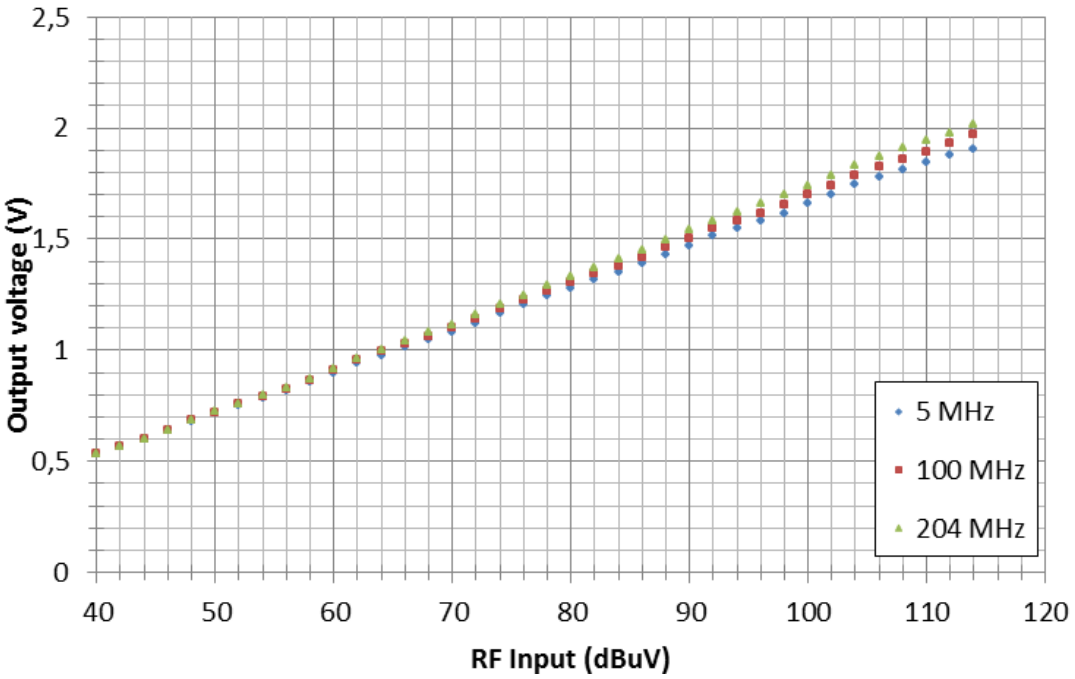

Figure 5.2 *RF-to-DC conversion of Detector A.*

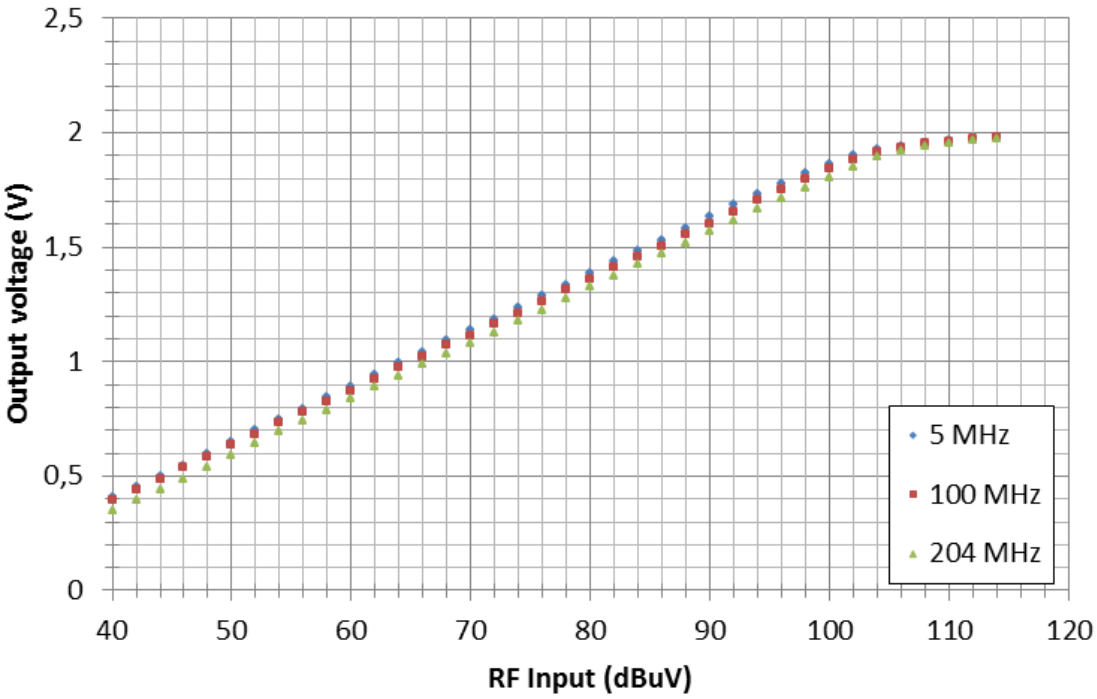

Figure 5.3. *RF-to-DC conversion of Detector B.*

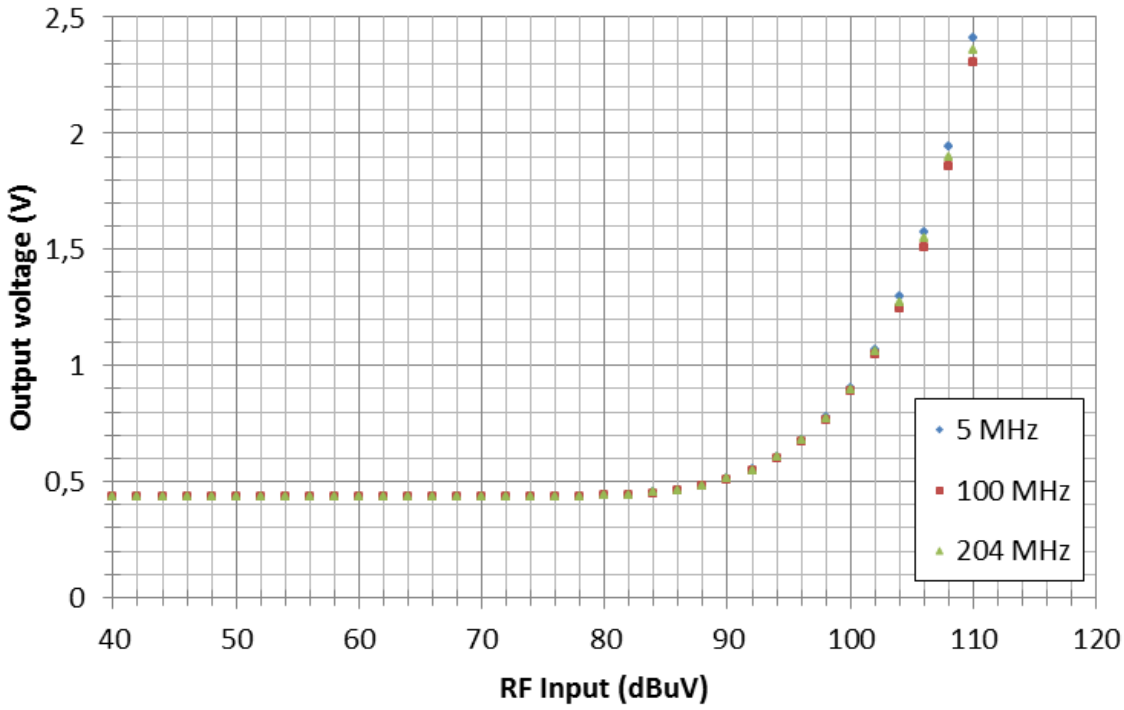

Figure 5.4. *RF-to-DC conversion of Detector C.*

5.1.2 Detector output voltage rise and fall times

The rise and fall times of the detectors were measured using the measurement setup of Figure 5.1, but the voltage meter was replaced with an oscilloscope. Also, the input RF signal was pulse modulated. The measurement results for the rise and fall times for a pulsed RF are presented in Table 5.2. The measurement results are only presented for a 100 MHz signal, although the response times were verified for the whole upstream bandwidth of 5-204 MHz. The variation in response times versus frequency was not significant.

Table 5.2. *Rise and fall times of the measured detectors.*

Sample	Type	Rise time	Fall time
Detector A	Logarithmic amplifier	264 ns	504 ns
Detector B	Logarithmic amplifier	328 ns	4300 ns
Detector C	Discrete design using an operational amplifier	744 us	976 us

Detector A exhibited the fastest rise and fall times. Detector B had a decent output voltage rise time, but a poor fall time. This suggests that if Detector B was utilized in a micronode, it might be too slow to meet the strict specification requirements. Detector C was observed to be the slowest with rise and fall times almost in the order of milliseconds. It is clearly not suitable for an RFoG application.

Based on the measurement results, Detector A was chosen to be used in the design. It exhibited the fastest rise and fall times and a good RF-to-DC transfer curve.

5.2 Laser turn-on and turn-off powers.

The input RF powers for which the laser turns on and off are determined by the comparator hysteresis circuit. The resistor values were chosen based on the measurement results for the RF-to-DC conversion of Detector A and applying equation (3.21) presented in Chapter 3.5.2. Figure 5.5 presents a diagram of the proposed device that was measured.

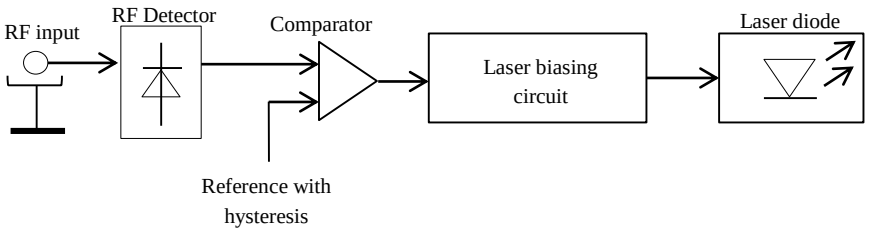

Figure 5.5. *A diagram of the device under test.*

The turn-on/turn-off input powers were measured by sweeping the input power with 1 dB steps, while monitoring the laser optical power using an oscilloscope. The behavior was measured in the whole DOCSIS 3.1 maximum upstream bandwidth of 5 – 204 MHz in 5 MHz steps. Figure 5.6 depicts the measurement setup and Figure 5.7 the obtained results.

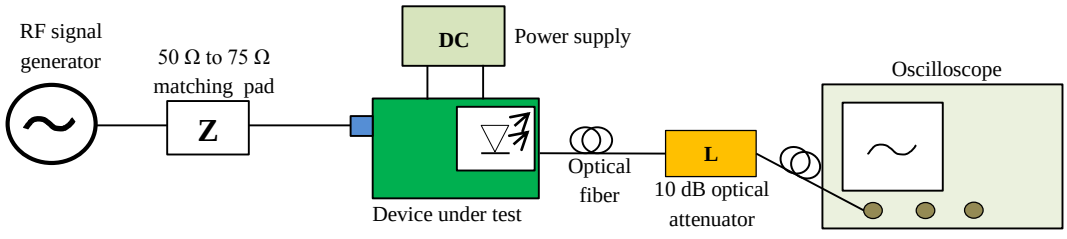

Figure 5.6. *Measurement setup for turn-on and turn-off powers.*

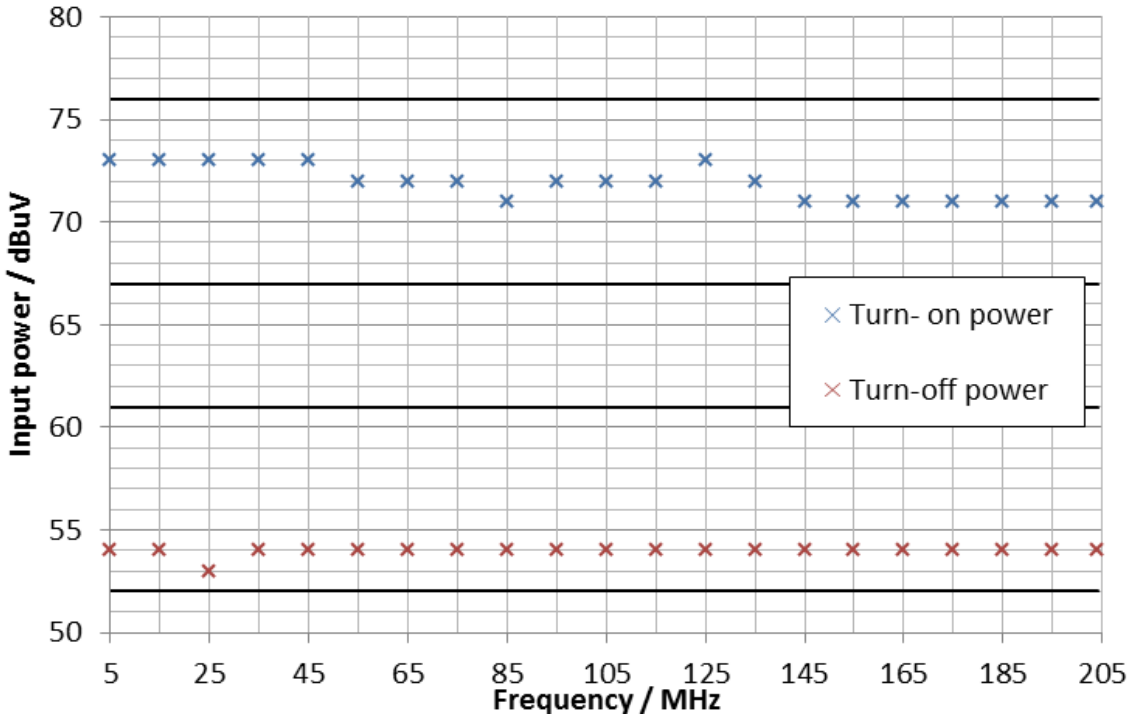

Figure 5.7. *Measurement results for laser turn-on and turn-off powers. Areas inside the black lines represent the specification requirements.*

The turn-on and turn-off powers lie within the required ranges. At the lower range of the upstream band, the laser turns on with 73 dBuV of input power. At the higher end of the band the turn on power is 71 dBuV. The turn-off power is 54 dBuV, with one measurement point being 53 dBuV.

Note that the measured design did not consist of a directional coupler presented in Figure 4.1 of Chapter 4. It would be required in a complete RFoG transmitter, because the main portion of the RF power would be guided to modulate the laser. The scope of this thesis was only to develop a fast switch on/switch off mechanism for the laser. With the usage of a directional coupler the actual input power fed to the detector would be less. By modifying the hysteresis circuit, the turn on and turn off powers can be moved to values, which take into account the difference produced by the coupler.

5.3 Laser turn-on and turn-off time delays

The turn-on and turn-off time delays of the prototype were measured using an oscilloscope. The oscilloscope was equipped with optical and electrical inputs. A pulsed signal was produced with an externally on-off modulated RF signal generator. The generated test signal was split to the oscilloscope and the device under test. The splitting of the test signal enabled the response time measurement: optical power is measured simultaneously with the pulsed RF signal. The diagram and a picture of the measurement setup

is presented in Figures 5.8 and 5.9, respectively. Table 5.3 summarizes the used test equipment.

Table 5.3. *Instruments used in the measurement setup.*

Instrument	Model
Oscilloscope	Tektronix CSA7154
RF generator	Marconi Instruments 10 kHz – 2,4 GHz multisource generator
Function generator	Tektronix AFG320 Arbitrary function generator

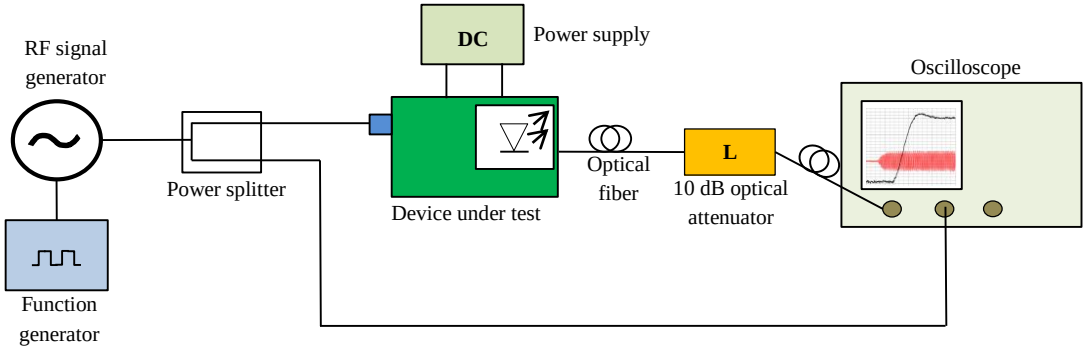

Figure 5.8. *A diagram of the measurement setup for laser rise and fall times.*

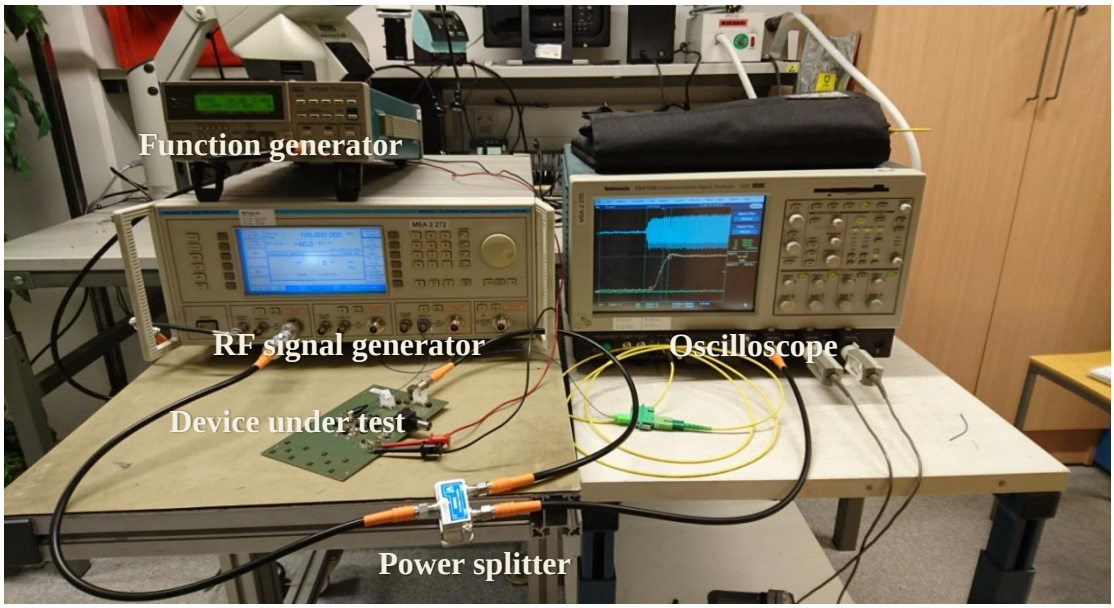

Figure 5.9. *Measurement setup for laser rise and fall times.*

Figure 5.10 presents two bursts of RF signal, and the turn-on and turn-off of the optical power.

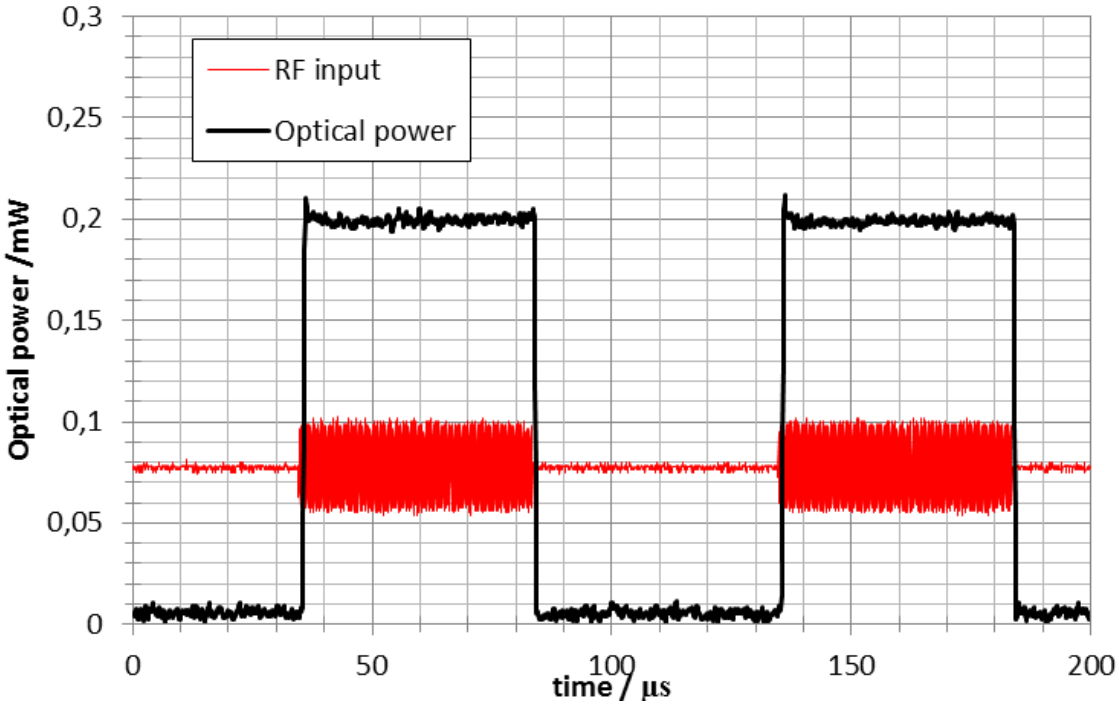

Figure 5.10. *Turn-on and turn-off of the transmitting laser.*

As seen, the laser is active only when an RF signal is present. This proves that the designed concept works as expected. The measured optical power is 0.2 mW. A 10 dB attenuator was placed between the laser and the oscilloscope as presented in Figure 5.8. Thus, the actual optical carrier power is 2 mW (~3 dBm). It is also noted that there is a slight overshoot, when the laser is turned on.

The measurement results for optical rise and fall times for 100 MHz input signal are presented in Figures 5.11 and 5.12, respectively. Note that the signal in the following graphs appear to be approximately 50 MHz rather than 100 MHz. However, it is due to aliasing.

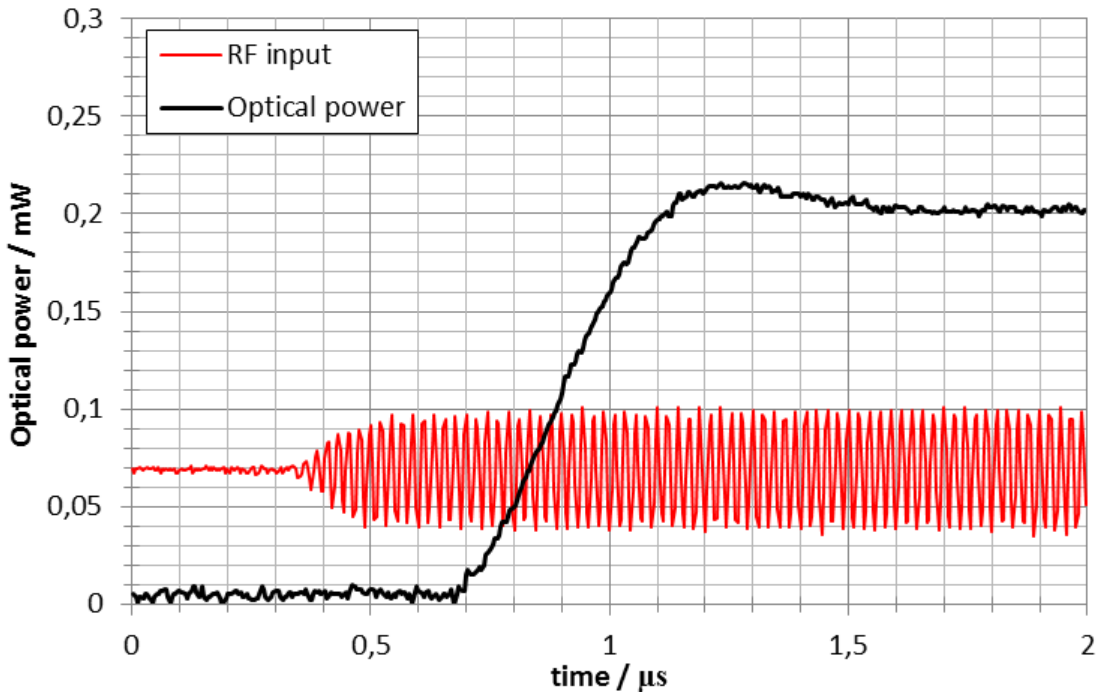

Figure 5.11. *Measured laser turn-on delay.*

The measured time delay from the application of RF to optical power reaching 90 % of its steady state value was measured to be 700 ns. The response time is measured from the instant that the envelope of the RF signal starts to rise. The envelope rises to the maximum value in approximately 250 ns. If the Marconi signal generator would have exhibited faster rise times for the RF envelope, the measured response time for the device could have been even shorter. It is noted, that optical power starts rising approximately 350 ns after the application. This corresponds to the response time of the detector-comparator combination.

Measurement result for the optical 10% to 90% rise time was 450 ns. The specified minimum time is 100 ns. The optical rise time is proportional to the slew rate of the operational amplifier. By using an op amp with a higher slew rate, smaller optical rise time could be achieved. There is a slight overshoot in the optical power, which dissipates approximately in 450 ns.

The turn-off time delay was measured using the same setup. Result for optical fall time is presented in Fig. 5.12.

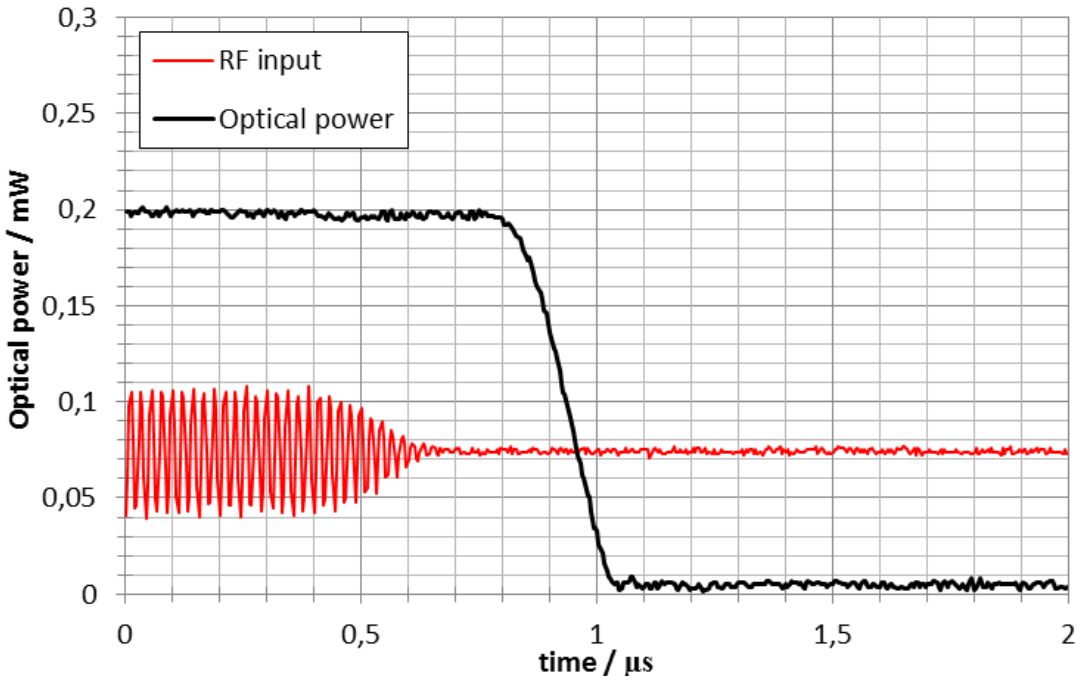

Figure 5.12. *Measured laser turn-off delay.*

The measured time delay from the removal of RF to 10 % optical power was measured to be 600 ns. If the time was measured from the instance that the RF signal has completely disappeared, the time would be 400 ns. The optical fall time from 90% to 10% optical power was measured to be 200 ns.

Table 5.4 summarizes the results regarding laser rise and fall times and compares them to the requirement.

Table 5.4. *A summary of measurement results for laser turn-on and turn-off times.*

Measurement	Measured	Requirement	Pass / Fail
Maximum time from application of RF to 90% optical power	700 ns	< 1.3 µs	Pass
Optical power 10% - 90 % rise time	450	100 ns – 1 µs	Pass
Maximum time from removal of RF to 10% optical power	600 ns	< 1.6 µs	Pass
Optical power fall time	200 ns	100 ns – 1 µs	Pass

The specification requirements for the response time and optical rise/fall times were met. The measured turn-on and turn-off response times were measured to be 600 ns and 1000 ns shorter than required in the specification.

5.4 Summary

Different detectors were measured and evaluated to find a suitable candidate for the final design. Detector A, the LT5537, excelled over the other two due to its fast response time and accurate RF-to-DC behavior over the 5 – 204 MHz bandwidth. Using the measurement results obtained for Detector A, the hysteresis circuit of the compactor was finalized.

The turn-on and turn-off behavior of the proposed device was measured after the most suitable detector was chosen. The obtained measurement results indicated that the requirements given in the SCTE RFoG specification were met. The obtained turn-on and turn-on time delays were significantly lower than the limits set by the specification. The device was able to turn on and turn off the laser diode with correct input power ranges.

The results indicate that the proposed laser driver architecture could be utilized in a commercial RFoG micronode product.

6. CONCLUSIONS

This thesis presented a concept that could be utilized as the laser bias control circuit in an RFoG micronode upstream transmitter. First, the reader was presented the basics of RFoG networks and the RFoG optical networking unit, the micronode. In order to familiarize the reader on the technology in hand, background theory was given on the physical phenomena, electrical components, and techniques utilized in the design.

The objective of this thesis was to develop and build a concept for a laser control circuit that could be utilized in Teleste corporations future micronode product. The proposed design consists of three building blocks: a detector, comparator and switching current regulation circuit. Different components and control solutions were compared and discussed. The best combination from the available detectors and comparators were chosen and realized together with the current control circuit.

Three different detectors were evaluated by measurements. Two of the detectors were logarithmic detectors and one a discrete solution utilizing Schottky diodes. The chosen detector was a LT5537 logarithmic detector, which excelled in response time compared to the others. Methods for current regulation were also discussed. The current regulation was implemented using an operational amplifier with negative feedback. The feedback utilized the built-in photodiode of the semiconductor laser. The laser bias current on/off switching was achieved by manipulating the voltage at the non-inverting input of the operational amplifier. Other switching methods were also discussed, but omitted from the final design.

The SCTE RFoG specification dictates that a micronode transmitter must turn on the transmitting semiconductor laser in 1.3 µs, when it senses an upstream signal in its input. When the signal is removed, the laser must turn off within 1.6 µs. The developed device met the turn-on and turn-off requirements set by the specification. The obtained laser turn-on and turn-off times were 700 ns and 600 ns, respectively. In addition, there are specifications for the input powers, which lead to laser turn-on and turn-off. These specifications were also met. The results proved that the designed laser driver circuit could be utilized in a commercial RFoG product. Also, the concept can be utilized in other applications, which require fast RF sensing.

Teleste Corporation offers several optical products, which incorporate upstream transmitters. However, they are designed to operate in HFC networks: the laser bias is always on regardless of the input RF power. The laser control architecture proposed in this thesis could be utilized in such product. By adding the combination of detector,

voltage comparator, and analog switch the optical power regulation circuit in such a product could be modified to exhibit the on/off behavior required in RFoG networks.

REFERENCES

[1] J. Chiddix, The Integration of Optical Fiber into Today's Cable Networks, Topical on Broadband Analog Optoelectronics: Devices and Systems, 1990. Monterey, CA, USA, July 23-25, 1990, IEEE, pp. 39-40.

[2] D. Stoneback, From Hybrid Fiber Coax to All-Fiber Networks, 2012 38th European Conference and Exhibition on Optical Communications (ECOC), Amsterdam, Netherlands, September 16-20, 2012, IEEE, pp. 1-3.

[3] J. Seidenber, Turning HFC into All-Fibre Networks, Broadband, Journal of the SCTE, Vol. 32, No. 3, pp. 58-62.

[4] Radio Frequency over Glass Fiber-to-the-Home Specification, Society of Cable Telecommunications Engineers, INC, SCTE 174 2010, 2010, 34 p. Available: https://www.scte.org/documents/pdf/Standards/SCTE%20174%202010.pdf.

[5] W. Ciciora, J. Farmer, D. Large, Modern Cable Television Technology, 1st ed. Morgan Kaufmann Publishers, California, 1999, 873 p.

[6] D. Raskin, D. Stoneback, Return Systems for Hybrid Fiber/Coax Cable TV Networks, 1st ed. Prentice Hall, New Jersey, 1998, 297 p.

[7] T. Rantanen, R&D Manager, Teleste Corporation, Turku, Interview 28.1.2016.

[8] CM-SP-PHYv3.1-I07-150910, Data-Over-Cable Service Interface Specifications DOCSIS® 3.1, Cable Television Laboratories, Inc, 2015, 244 p.

[9] S. Kulkarni, L. Yu Sr, RFoG ROI in Rural Environments, Aurora Networks, Inc, web page. Available (accessed 2.12.2015): http://www.pace.com/Documents/Whitepapers/Networks/WhitePaper020_RevA_Rural-RFoG-ROI.pdf.

[10] H. Young, R. Freedman, University Physics, 11th ed. Pearson Education, Inc, San Fransisco, 2004, 1714 p.

[11] D.J. Sterling, Technician's Guide to Fiber Optics, 3rd ed. Delmar, 1999, 345 p.

[12] F.L. Pedrotti, L.S. Pedrotti, Introduction to Optics, 2nd ed. Prentice Hall, New Jersey, USA, 1990, 602 p.

[13] RF and Microwave Fiber-Optics, Emcore Corporation, web page. Available (accessed 2.12.2015): http://www.emcore.com/wp-content/uploads/RF-and-Microwave-Fiber-Optic-Design-Guide.pdf.

[14] C. Garrett, The Optical Maser, Electrical Engineering, Vol. 80, No. 14, 1961, pp. 248-251.

[15] W. Heitler, The Quantum Theory of Radiation, 3rd ed. Oxford University Press, New York, USA, 1954, 430 p.

[16] W. Stephens, T. Joseph, System Characteristics of Direct Modulated and Externally Modulated RF Fiber-optic Links, Journal of Lightwave technology, Vol. 5, No. 3, 1987, pp. 380-387.

[17] LM741 Operational Amplifier, Texas Instruments, SNOSC25D, October 2015, 18 p. Available: http://www.ti.com/lit/ds/symlink/lm741.pdf.

[18] S. Franco, Design With Operational Amplifiers and Analog Integrated Circuits, 3rd ed. McGraw-Hill, New York, 2002, 658 p.

[19] Op Amp and Comparators – Don't Confuse Them! Texas Instruments, Application report, SLOA067, Sept. 2001, 13 p.

[20] LMx93-N, LM2903-N Low-Power, Low-Offset Voltage, Dual Comparators, Texas Instruments, SNOSBJ6F, Dec. 2014, 29 p. Available: http://www.ti.com/lit/ds/symlink/lm193-n.pdf.

[21] LT1720/LT1721 Dual/Quad, 4.5ns, Single Supply 3V/5V Comparators with Rail-to-Rail Outputs, Linear Technology, 28 p. Available: http://cds.linear.com/docs/en/datasheet/17201fc.pdf.

[22] F. Maloberti, Understanding Microelectronics: A Top-Down Approach, John Wiley & Sons, West Sussex, United Kingdom, 2012, 656 p.

[23] L. Frenzel, RF Detectors for Wireless Devices, Analog Devices, web page. Available (accessed 22.11.2015): http://www.analog.com/media/en/technical-documentation/frequently-asked-questions/201551981Detector_FAQ.pdf.

[24] D. Pozar, Microwave Engineering, 4th ed. John Wiley & Sons, Inc, USA, 2012, 756 p.

[25] HSMS-282X Surface Mount RF Schottky Barrier Diodes, Avago Technologies, November 26, 2014, 15 p. Available: http://www.avagotech.com/docs/AV02-1320EN.

[26] Data Sheet AD8307, Low Cost, DC to 500 MHz, 92 dB Logarithmic Amplifier, Analog Devices, 9/15, 24 p. Available: http://www.analog.com/media/en/technical-documentation/data-sheets/AD8307.pdf.

[27] LT5537 Wide Dynamic Range RF/IF Log Detector, Linear Technology, 2005, 16 p. Available: http://cds.linear.com/docs/en/datasheet/5537fa.pdf.

[28] MC33172 MC35172 Low Power Dual Bipolar Operational Amplifiers, STMicroelectronics, 01-Jul-2008, 9 p. Available: http://www.mouser.com/ds/2/389/CD00000476-250861.pdf.